Measuring isotropic cosmic birefringence with LiteBIRD

Patricia Diego-Palazuelos
on behalf of LiteBIRD's Cosmic Birefringence Project Study Group
M. Bortolami, E. de la Hoz, J. Errard, A. Gruppuso, B. Jost, R. Sullivan

International Workshop on Multi-probe approach to Wavy Dark Matter
Korea University, Seoul
Nov 30 - Dec 2 2023

ALP coupling to electromagnetism

ALP can couple to EM through a Chern-Simons interaction

$$\mathcal{L} = -\frac{1}{2}\partial^\mu\phi\partial_\mu\phi - V(\phi) - \frac{1}{4}F_{\mu\nu}F^{\mu\nu} + \frac{1}{4}g_{\phi\gamma}\phi F_{\mu\nu}\tilde{F}^{\mu\nu}$$

Rotation of the plane of linear polarization clockwise on the sky

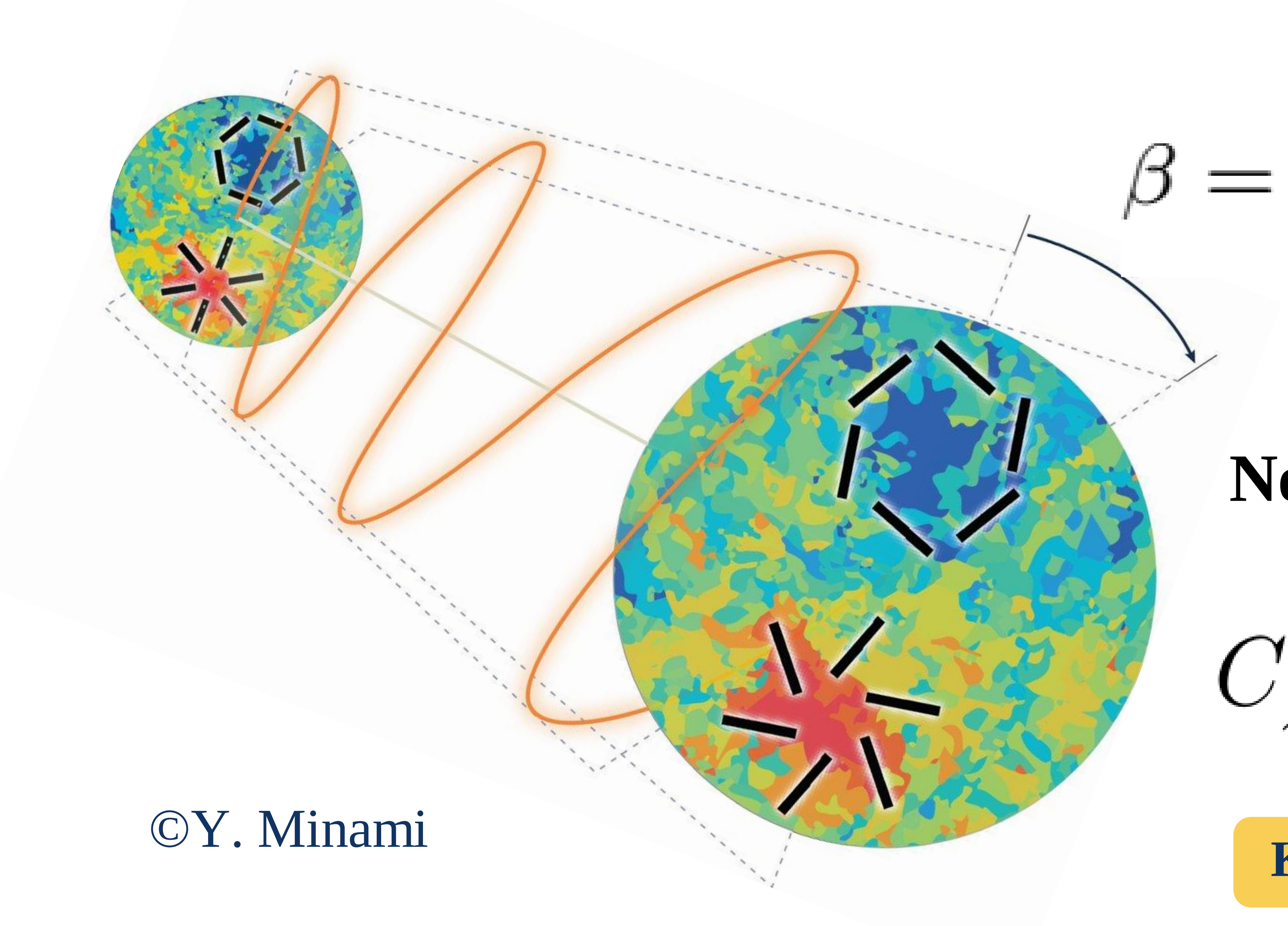

©Y. Minami

$$\beta = -\frac{1}{2}g_{\phi\gamma}\int\frac{\partial\phi}{\partial t}dt$$

Non-null CMB *EB* correlation

$$C_\ell^{EB,\mathrm{o}} = \frac{1}{2}\tan(4\beta)\left(C_\ell^{EE,\mathrm{o}} - C_\ell^{BB,\mathrm{o}}\right)$$

Komatsu Nat. Rev. Phys. 2022

ALP coupling to electromagnetism

ALP can couple to EM through a Chern-Simons interaction

$$\mathcal{L} = -\frac{1}{2}\partial^\mu\phi\partial_\mu\phi - V(\phi) - \frac{1}{4}F_{\mu\nu}F^{\mu\nu} + \frac{1}{4}g_{\phi\gamma}\phi F_{\mu\nu}\tilde{F}^{\mu\nu}$$

Rotation of the plane of linear polarization clockwise on the sky

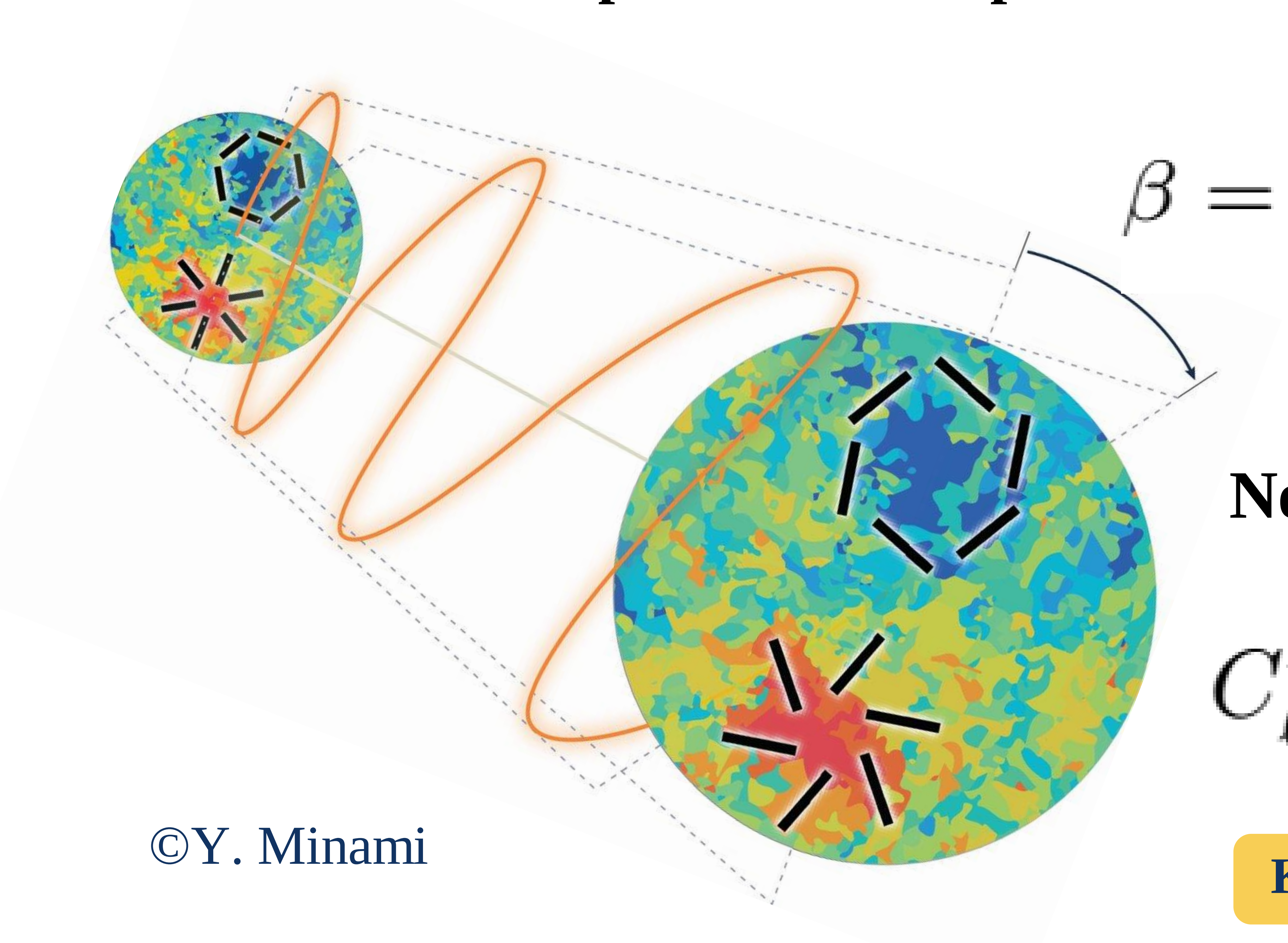

©Y. Minami

$$\beta = -\frac{1}{2}g_{\phi\gamma}\int\frac{\partial\phi}{\partial t}dt$$

Non-null CMB *EB* correlation

$$C_\ell^{EB,o} = \frac{1}{2}\tan(4\alpha + 4\beta)\left(C_\ell^{EE,o} - C_\ell^{BB,o}\right)$$

Komatsu Nat. Rev. Phys. 2022

Miscalibration of the detector's polarization angle

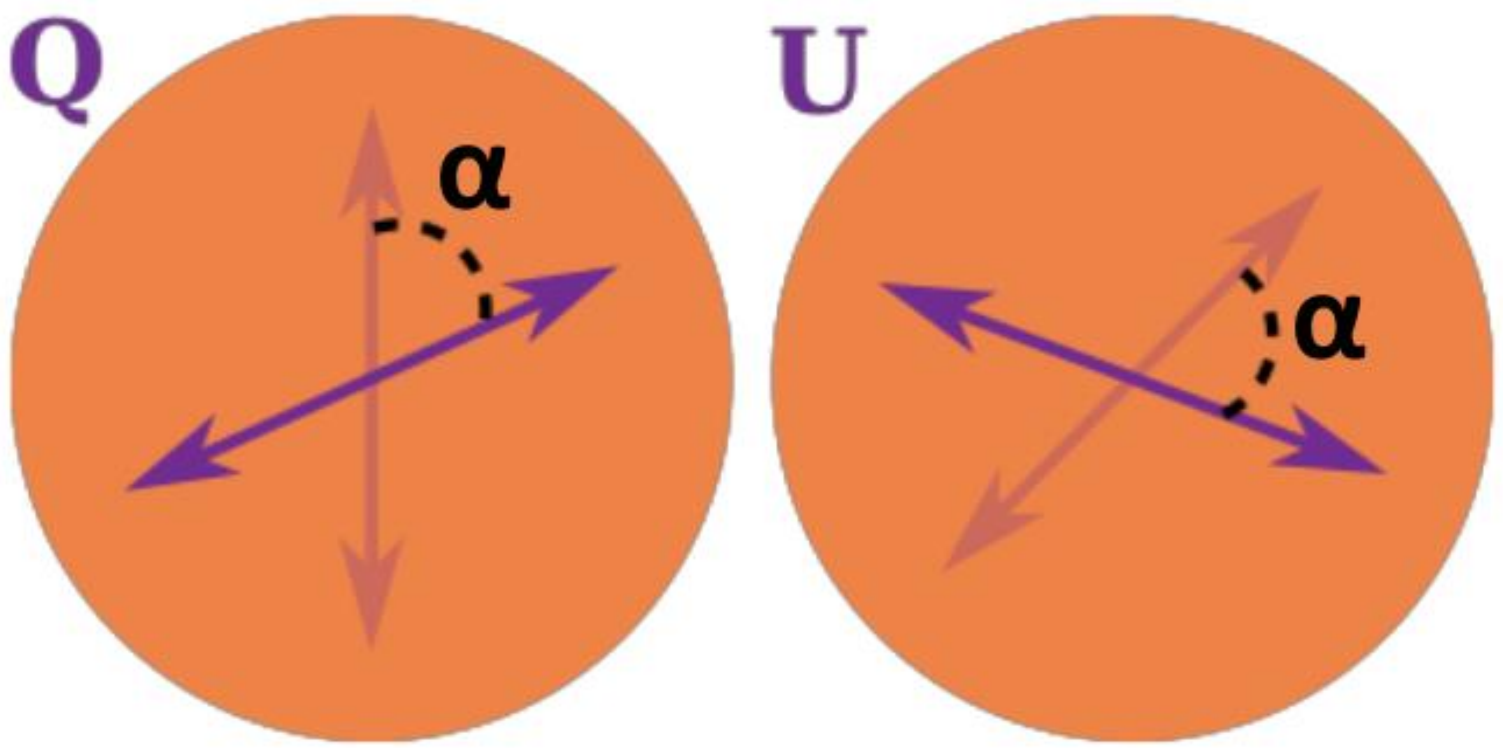

Krachmalnicoff+ JCAP 2022

Unknown α miscalibration
Completely degenerate with β

Calibrating against Galactic foregrounds

$$\beta = -\frac{1}{2} g_{\phi\gamma} \int \frac{\partial \phi}{\partial t} dt$$

Galactic emission not significantly rotated by β
Use foregrounds as our calibrator

Minami+ PTEP 2019

$$C_\ell^{EB,\mathrm{o}} = \frac{\tan(4\alpha)}{2}\left(C_\ell^{EE,\mathrm{o}} - C_\ell^{BB,\mathrm{o}}\right) + \frac{1}{\cos(4\alpha)} C_\ell^{EB,\mathrm{fg}} + \frac{\sin(4\alpha)}{2\cos(4\alpha)}\left(C_\ell^{EE,\mathrm{cmb}} - C_\ell^{BB,\mathrm{cmb}}\right)$$

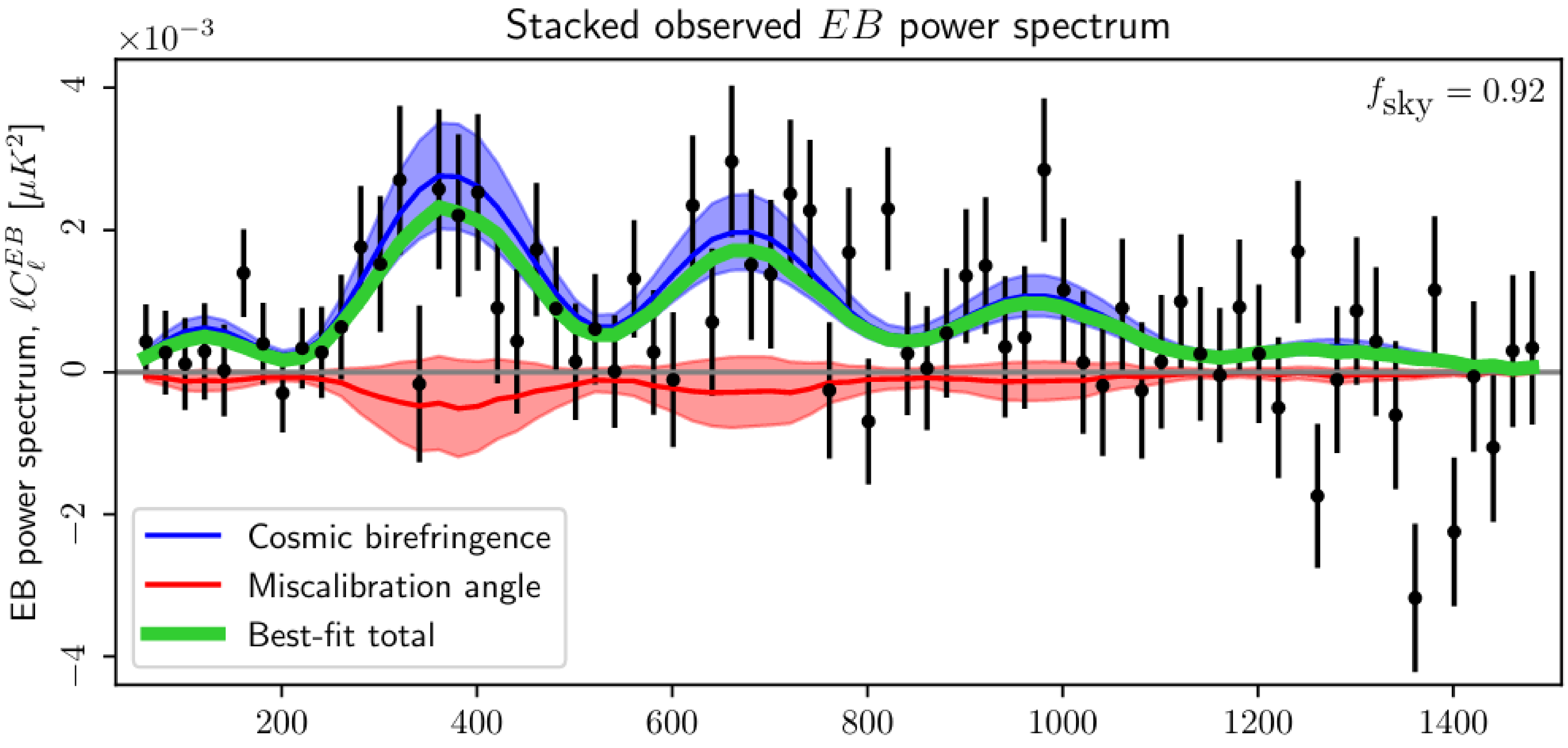

Model the *EB* correlation of Galactic synchrotron and dust emissions

Clark+ ApJ 2021

Tightest constraint to date (3.6σ)

$$\beta = 0.342^\circ \,{}^{+0.094^\circ}_{-0.091^\circ}$$

from the joint analysis of *Planck* and WMAP data

Eskilt & Komatsu PRD 2022

LiteBIRD overview

- Lite (Light) satellite for the study of *B*-mode polarization and Inflation from cosmic background Radiation Detection
- JAXA's L-class mission selected in May 2019
- Expected launch in late 2032 (JFY) with JAXA's H3 rocket
- **All-sky 3-year survey**, from Sun-Earth Lagrangian point L2
- Large frequency coverage (**40–402 GHz**, 15 bands) at **70–18 arcmin** angular resolution for precision measurements of the **CMB *B*-modes**
- Final combined sensitivity: **2.2 μK·arcmin**

LiteBIRD PTEP 2023

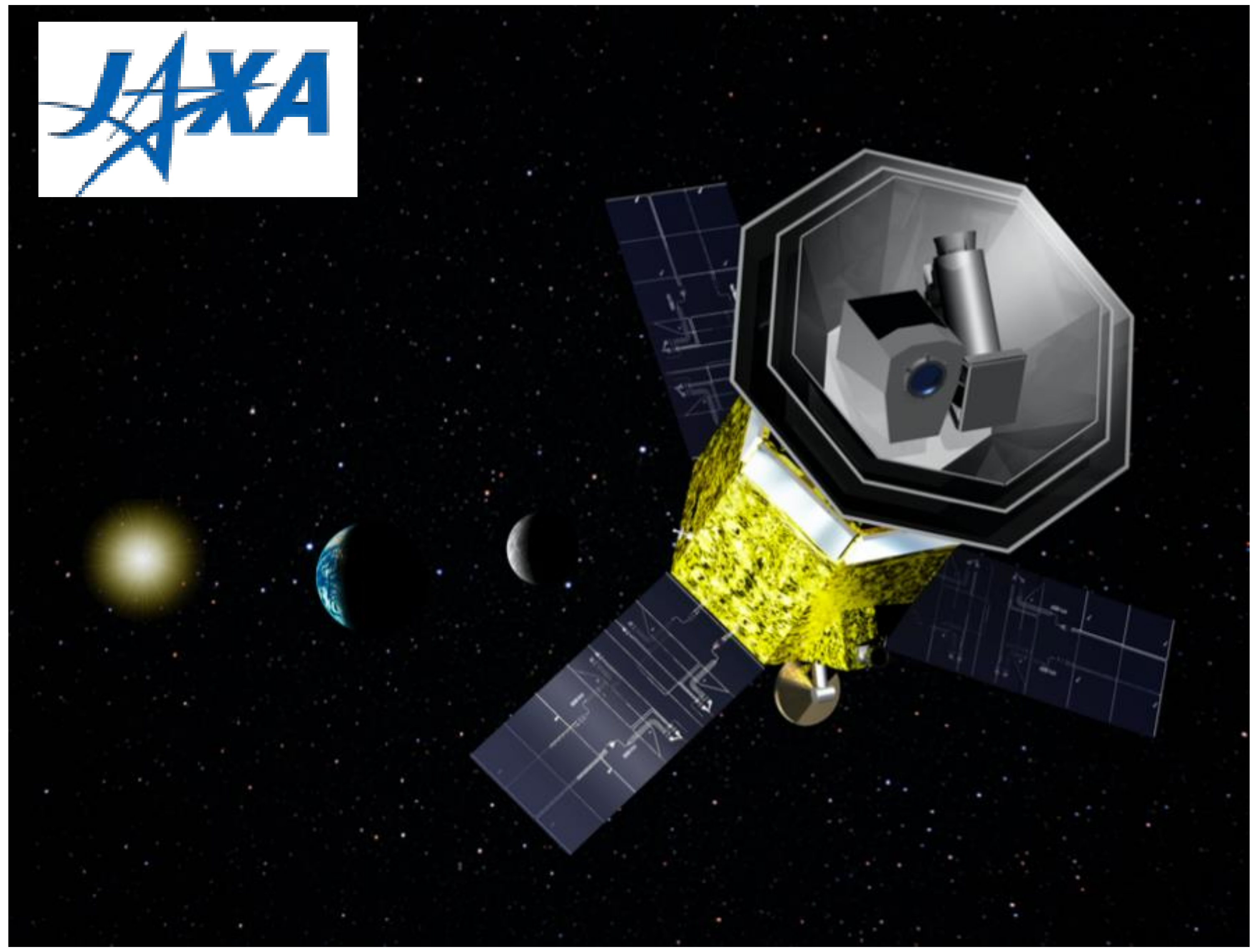

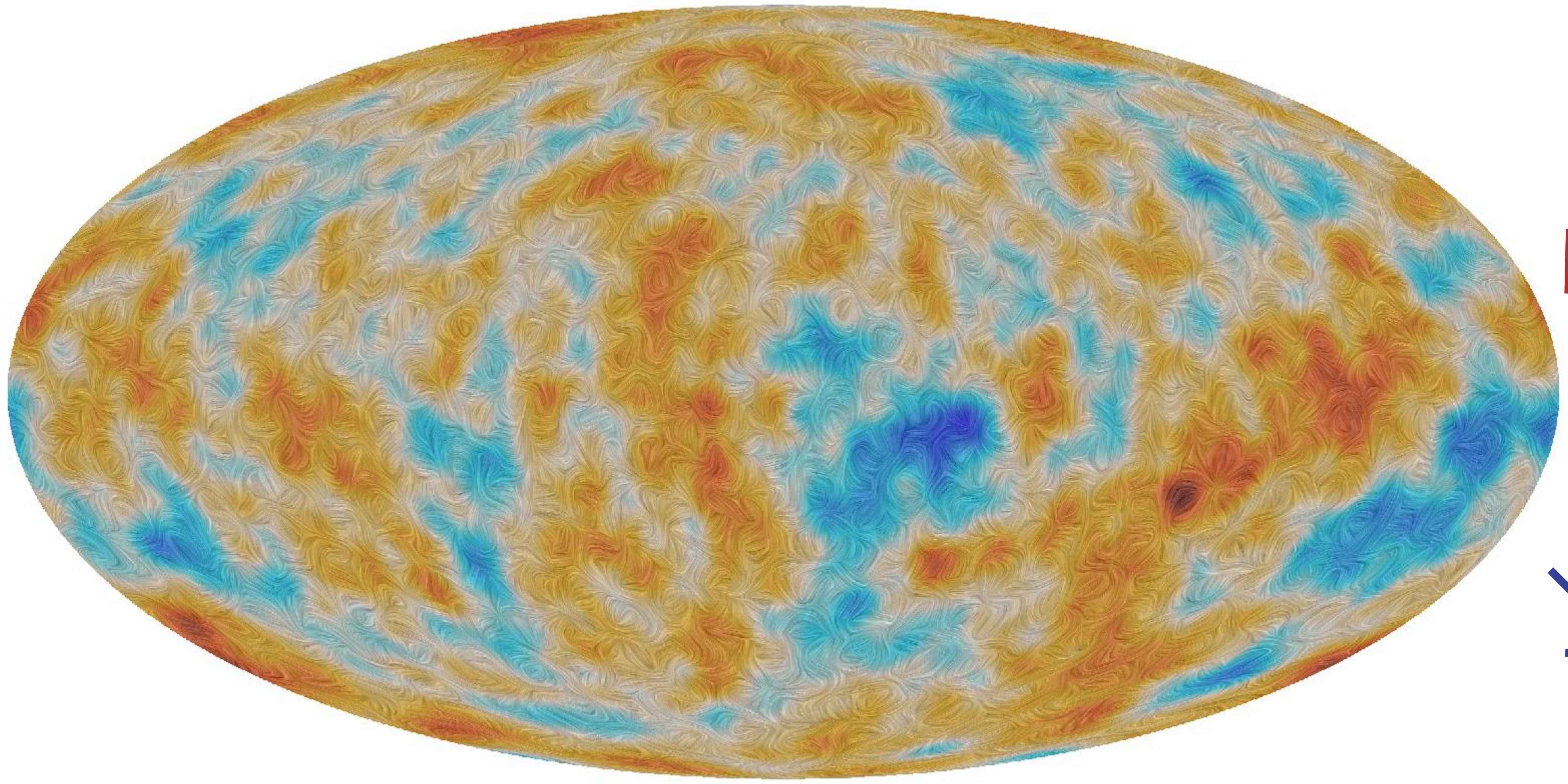

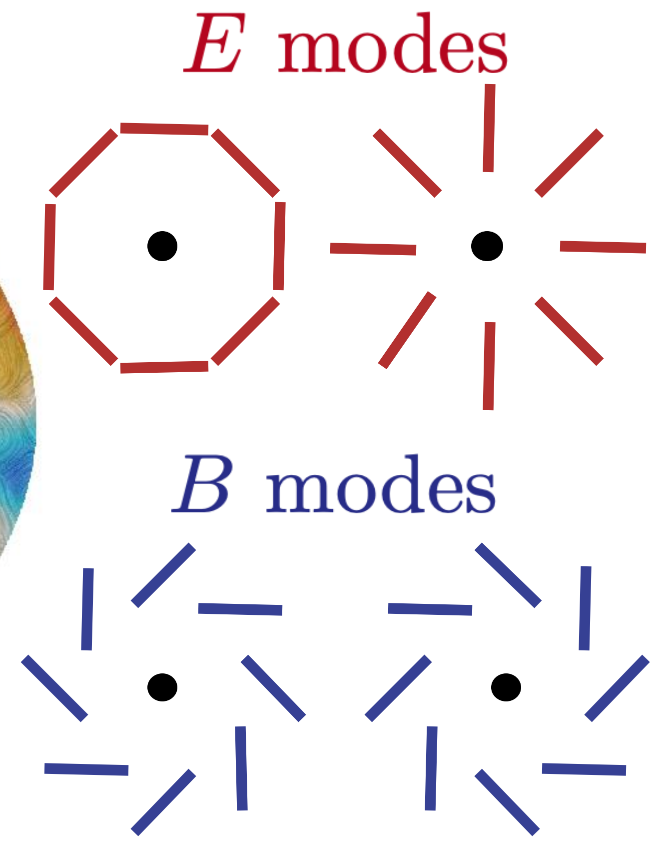

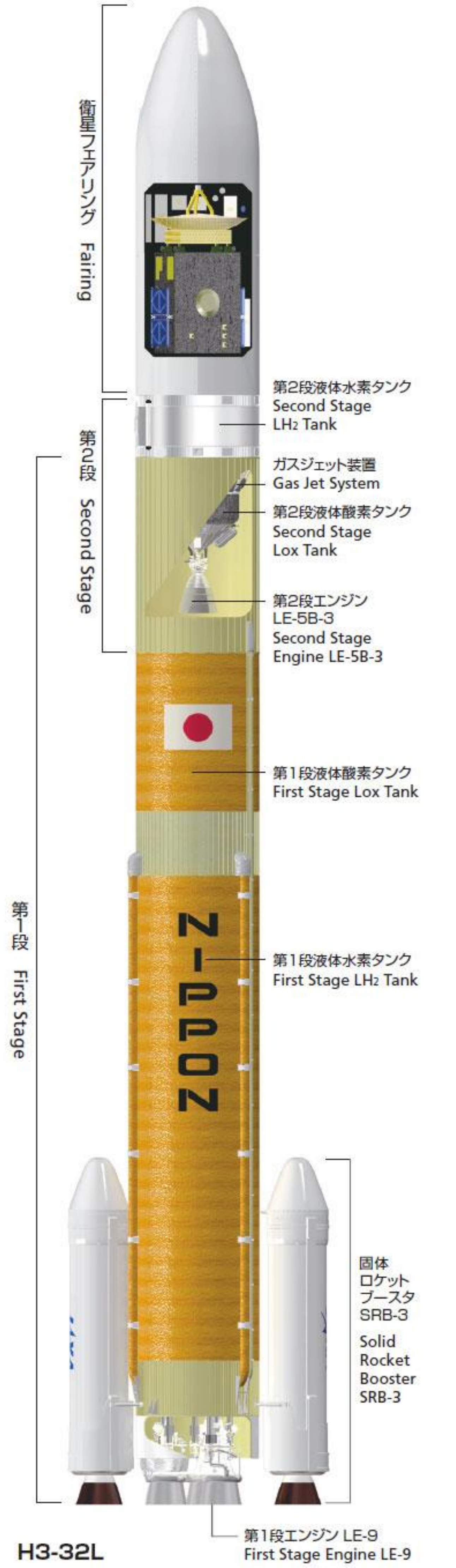

LiteBIRD main scientific objectives

- Definitive search for the **B-mode signal** from **cosmic inflation** in the CMB polarization
  - Making a discovery or ruling out well-motivated inflationary models
  - Insight into the quantum nature of gravity
- The inflationary (i.e. primordial) B-mode power is
- proportional to the **tensor-to-scalar ratio, r**
- Current best constraint: $r < 0.032$ (95% C.L.)
  (Tristram+ 2021, combining BK18 and Planck PR4)
- LiteBIRD will improve current sensitivity on r by a factor ~50
- L1-requirements (no external data):
  - For $r = 0$, **total uncertainty of $\delta r < 0.001$**
  - For $r = 0.01$, 5σ detection of the reionization ($2 < \ell < 10$) and recombination ($11 < \ell < 200$) peaks independently
- Huge discovery impact (evidence for inflation, knowledge of its energy scale, …)

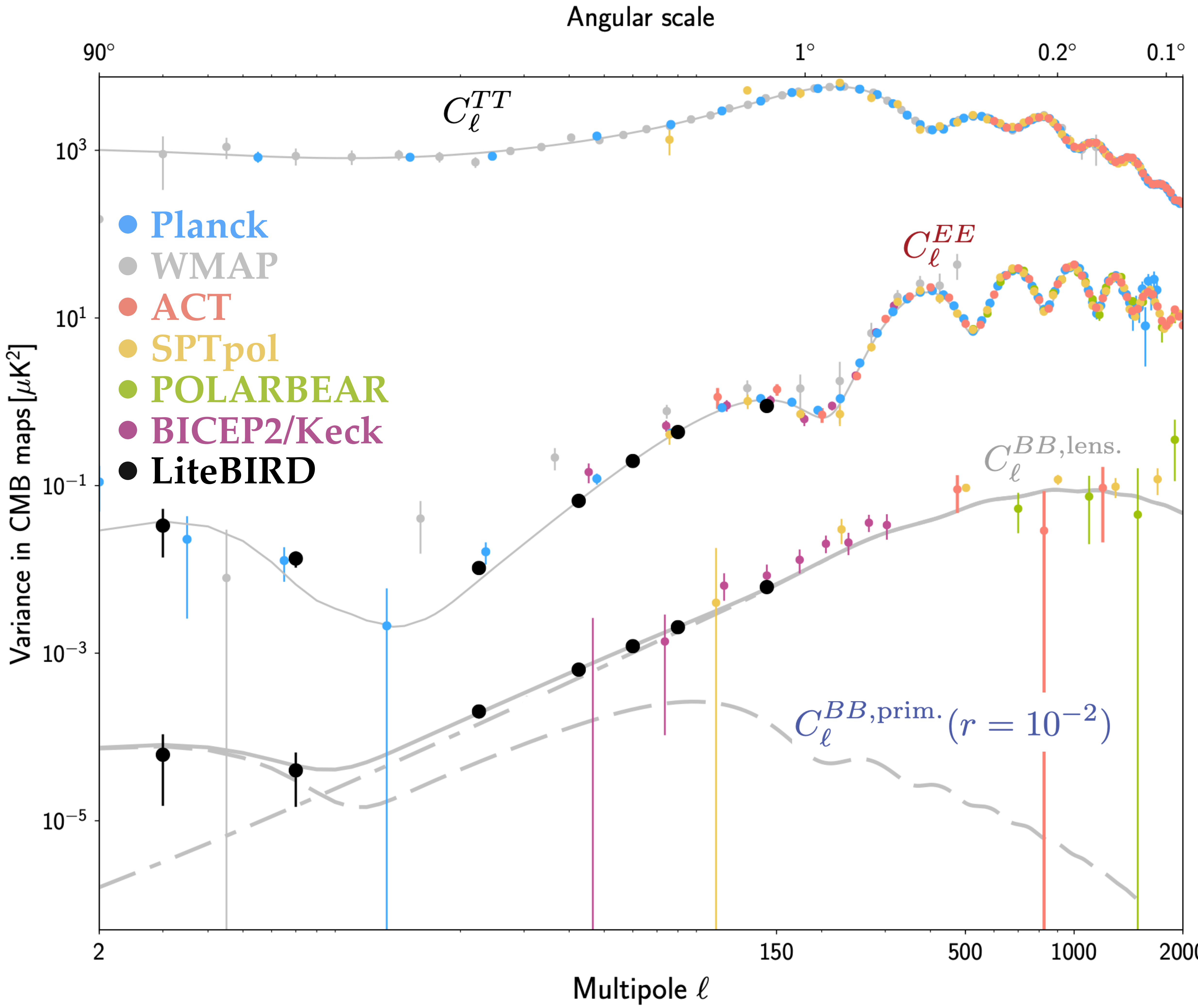

LiteBIRD spacecraft overview

- **3 telescopes** are used to provide the **40-402 GHz** frequency coverage
  1. **LFT** (low frequency telescope)
  2. **MFT** (middle frequency telescope)
  3. **HFT** (high frequency telescope)
- Multi-chroic transition-edge sensor (TES) **bolometer arrays** cooled to **100 mK**
- Polarization modulation unit (PMU) in each telescope with **rotating half-wave plate** (HWP), for 1/*f* noise and systematics reduction
- Optics cooled to **5 K**

- Mass: 2.6 t
- Power: 3.0 kW
- Data: 17.9 Gb/day

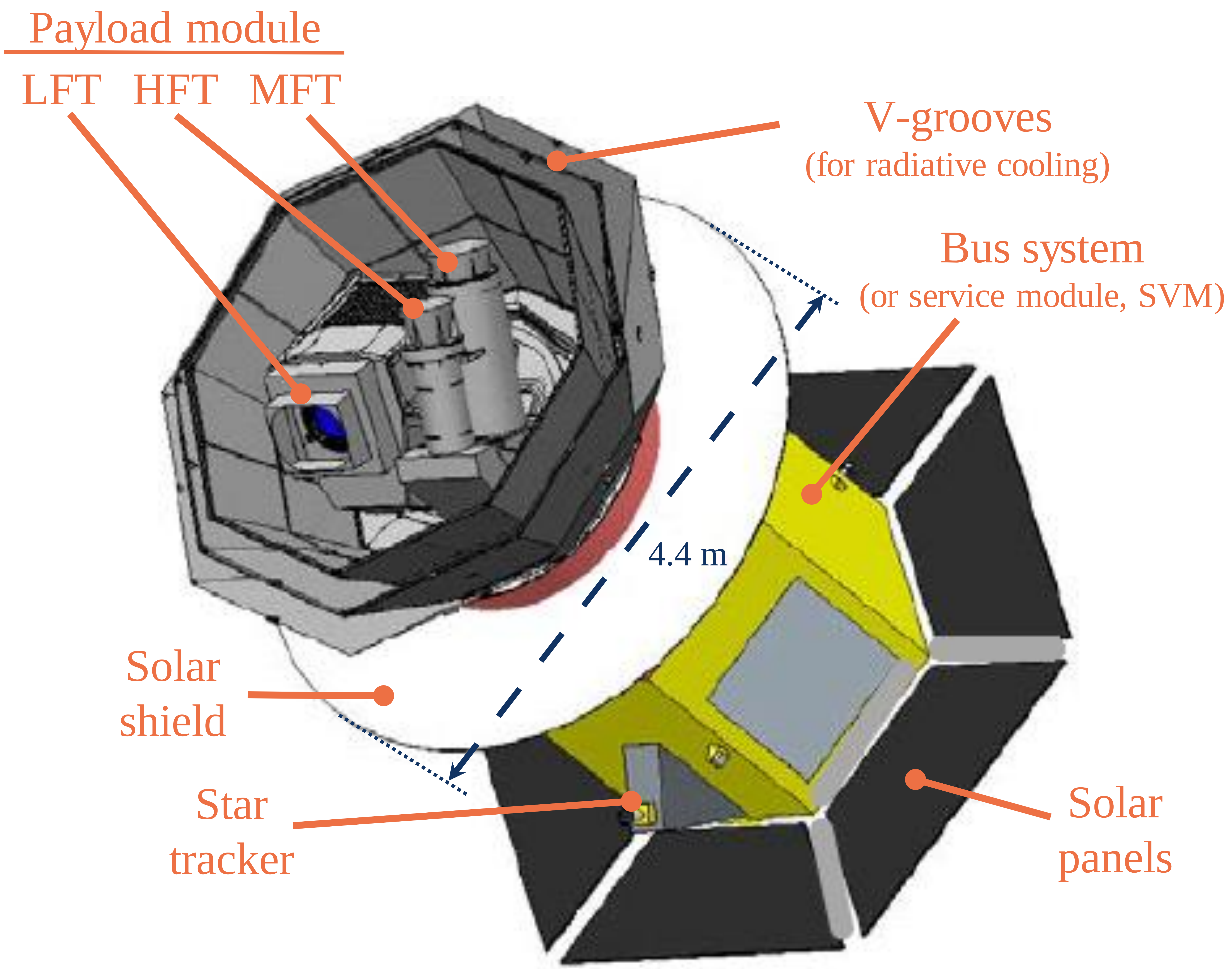

LiteBIRD as a birefringence probe

Precision measurement of *EB*

Wide frequency range
- Efficient component separation
- Improve synchrotron and dust models
- Cross-correlation of low and high frequencies reduces the impact of *EB* mismodeling

Full-sky coverage
- *EB* around the reionization peak probes the ALP mass and can distinguish between different ALP and early dark energy models

High signal-to-noise detections of β are possible with >20 arcmin resolutions

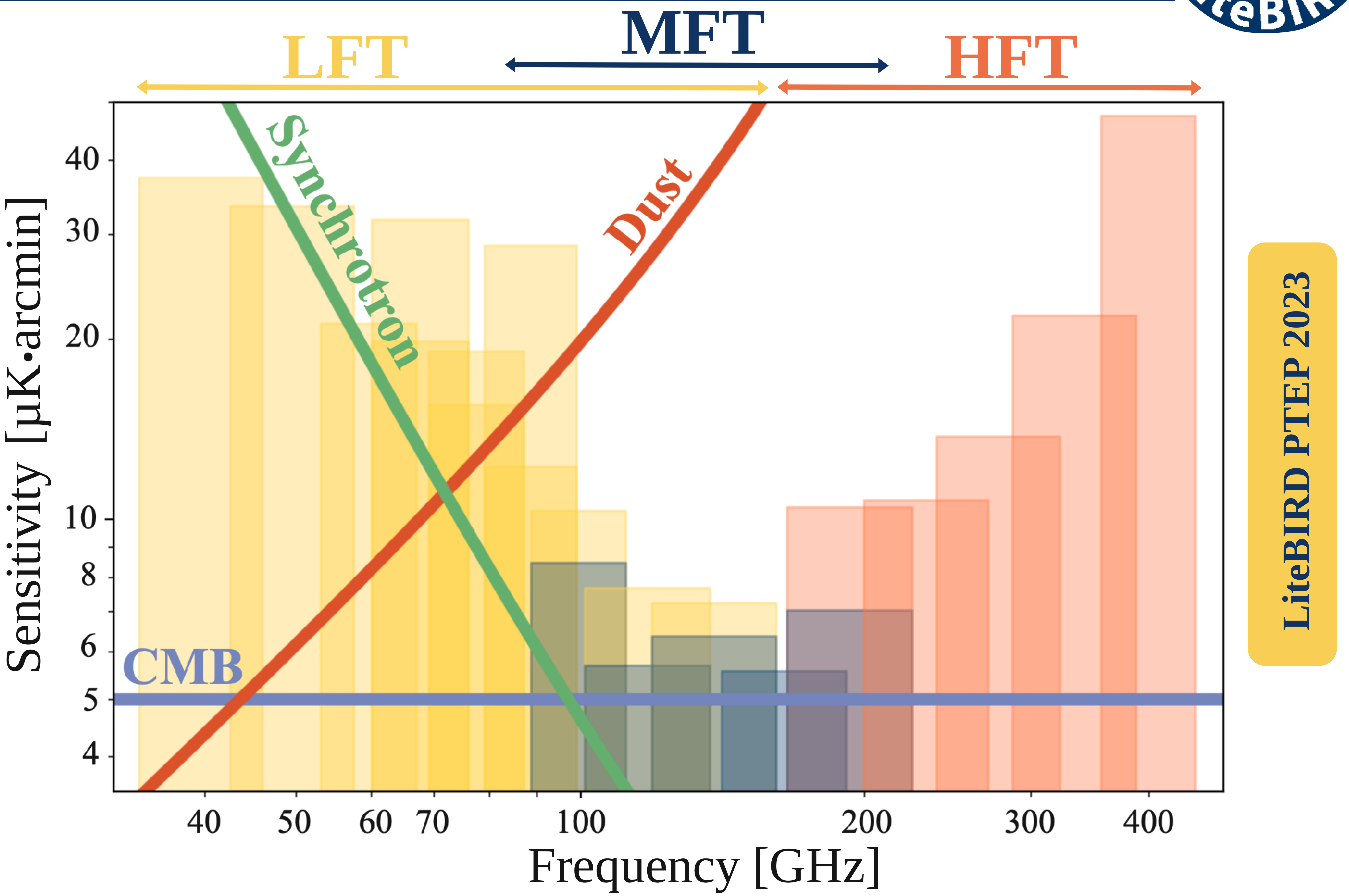

Projected **polarization sensitivities** for a **3-year full-sky survey**
- Best of 4.6 μK·arcmin @ 119 GHz
- Cosmic-variance-limited measurement of *E* modes at low multipoles

Analysis pipelines

Frequency maps

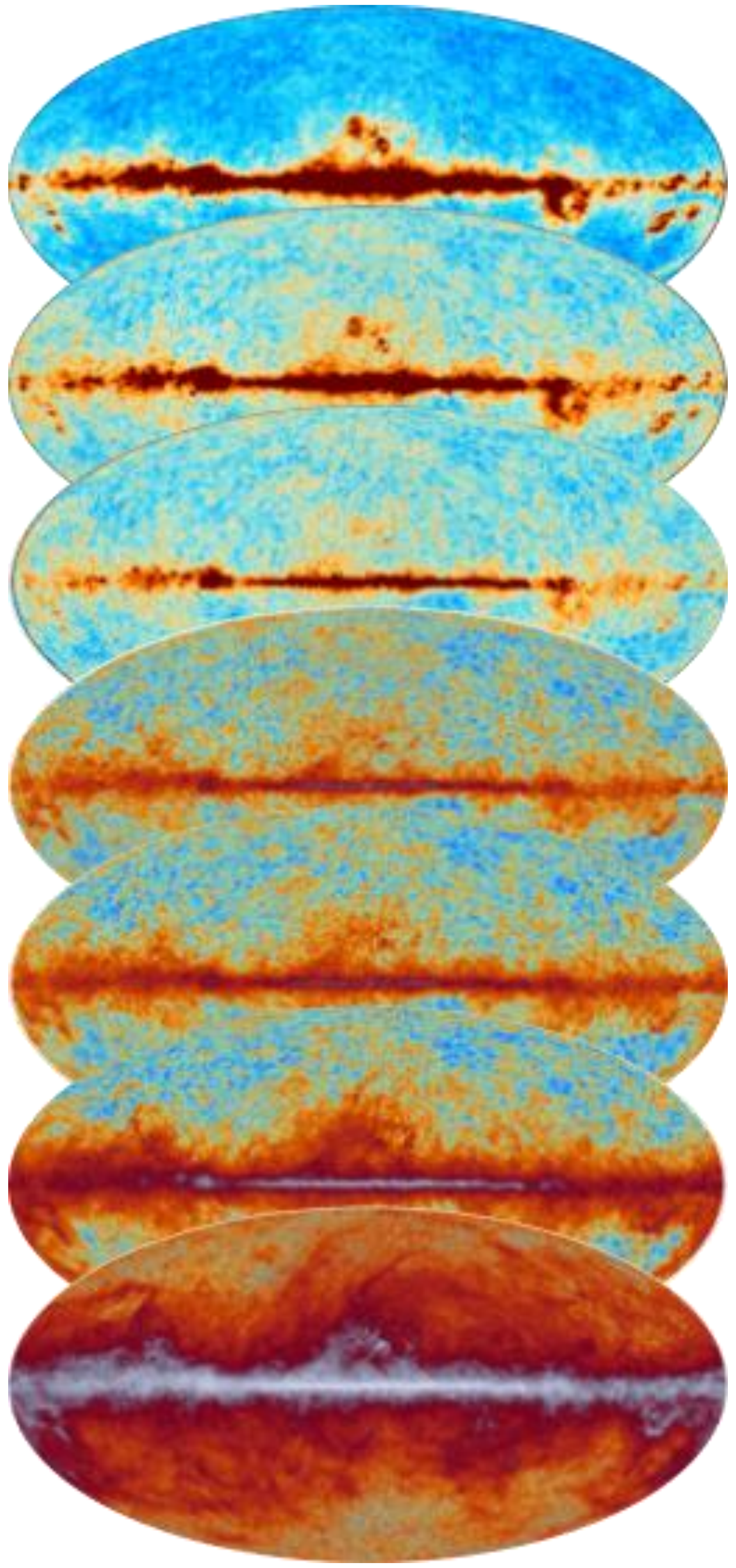

+ synch & dust model

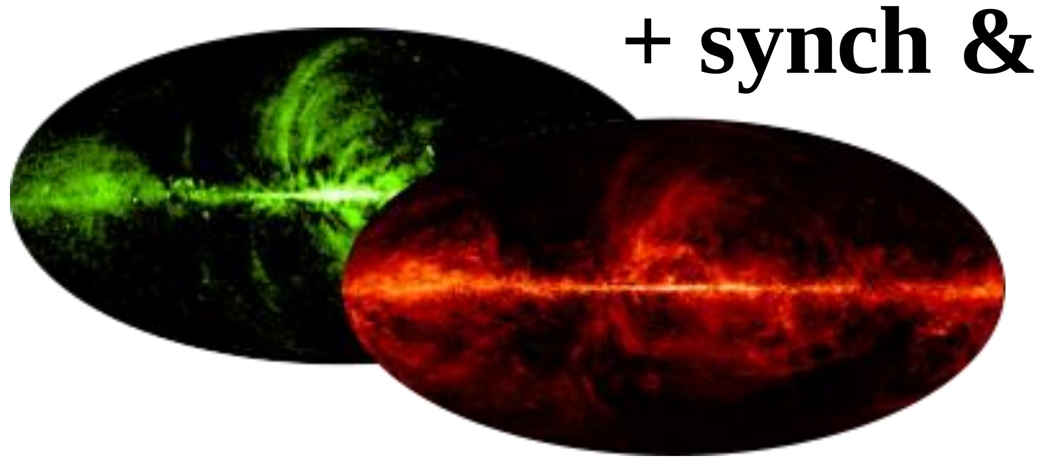

MK technique

α_i, β

Analysis pipelines

Frequency maps

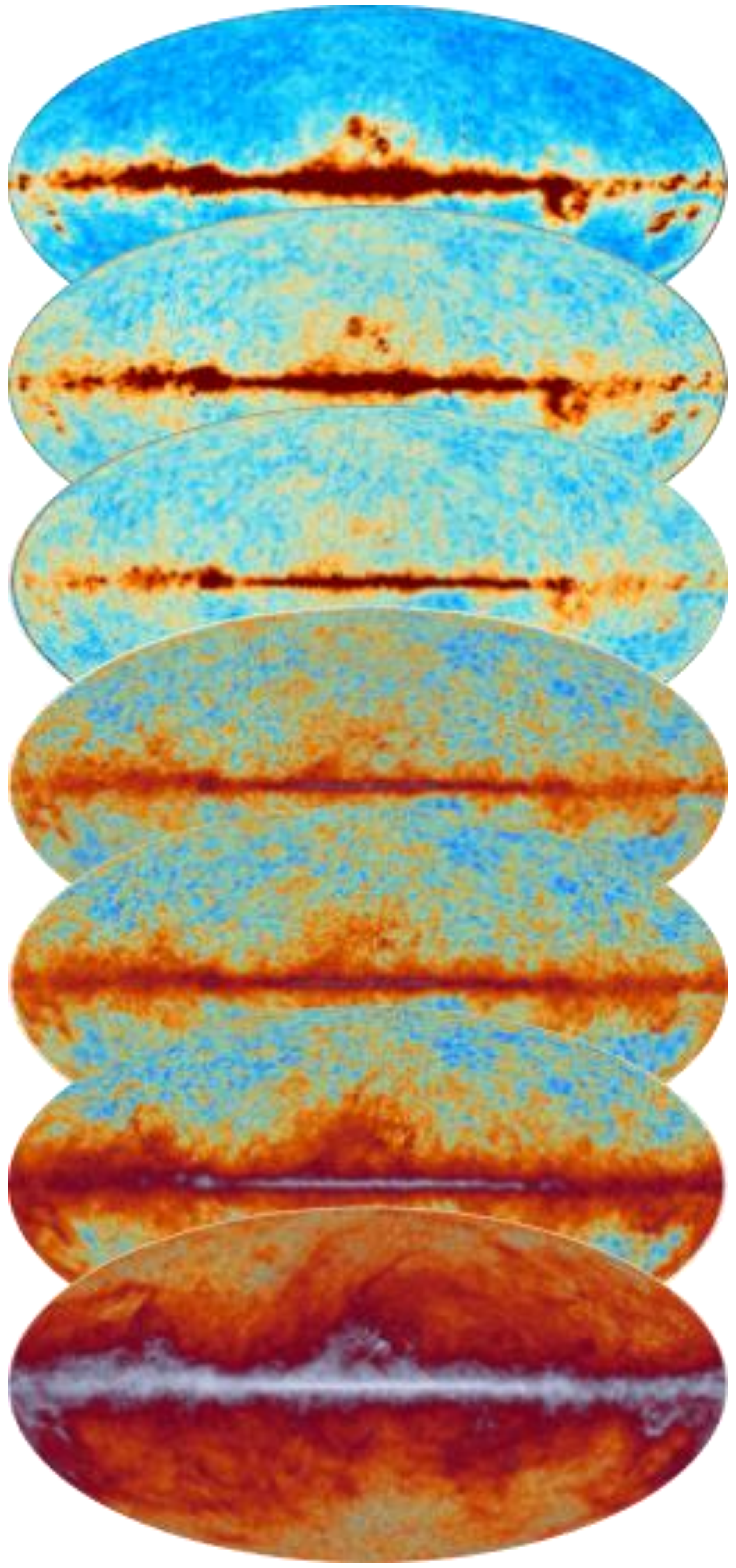

+ synch & dust model

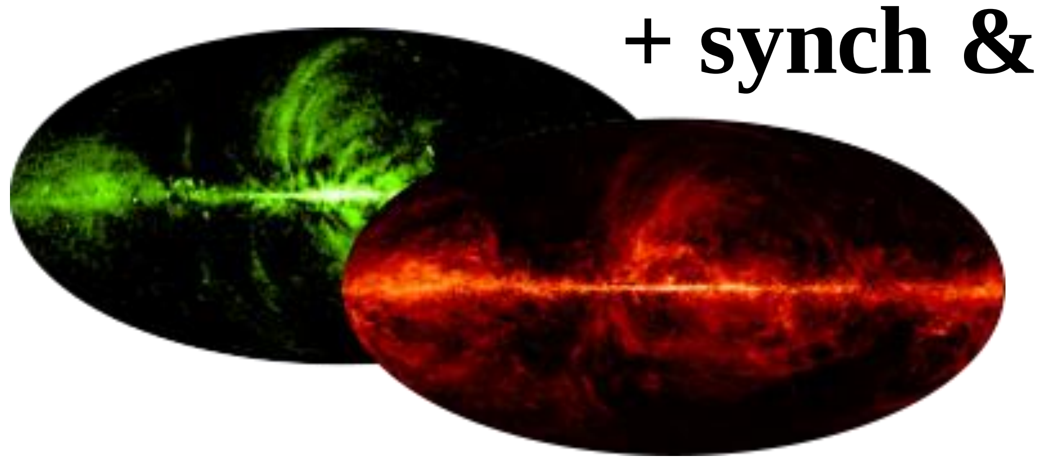

MK technique

Standard component separation

- Parametric SED

CMB

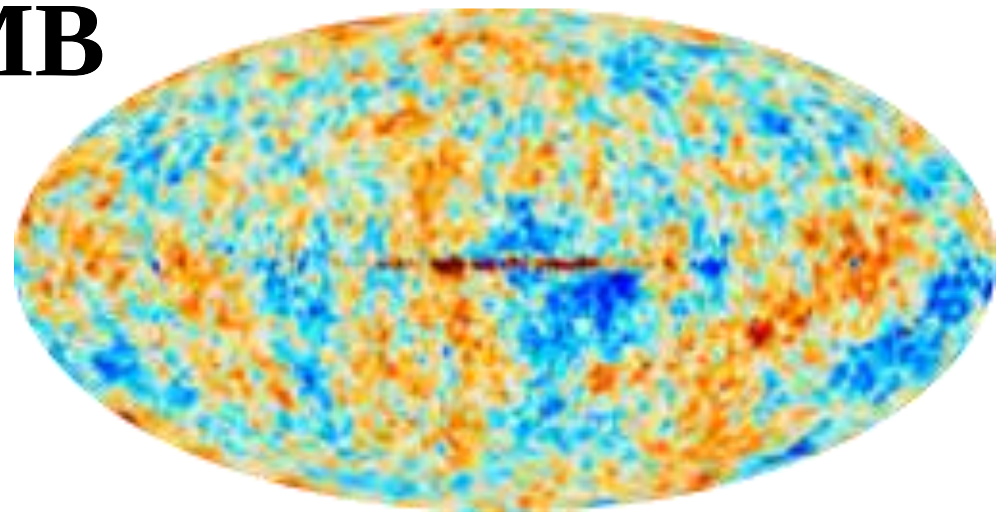

$\langle\alpha_i\rangle + \beta$ rotated

α_i, β

β from CMB

Harmonic space
D-estimator

Real space
Peak stacking

Analysis pipelines

Frequency maps

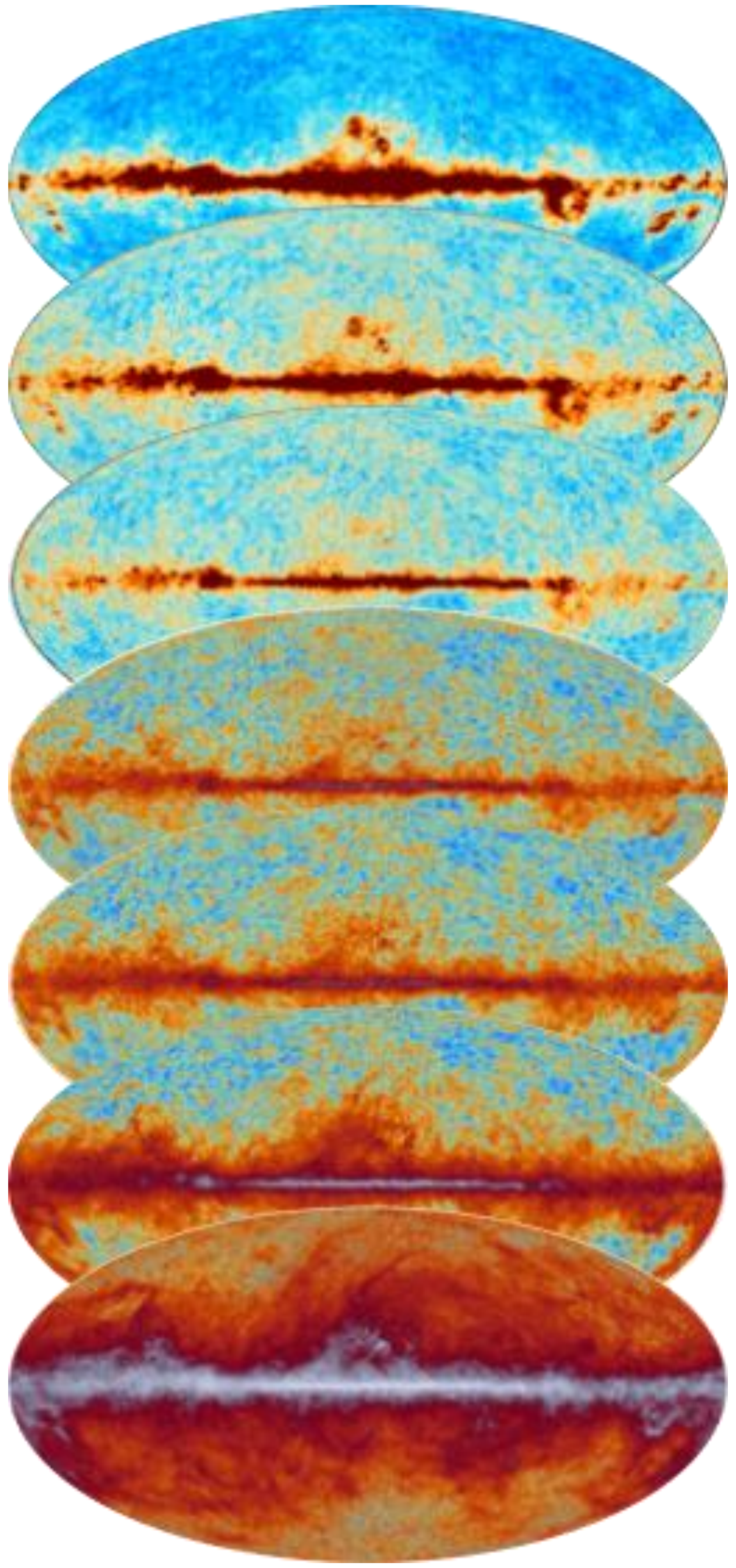

+ synch & dust model

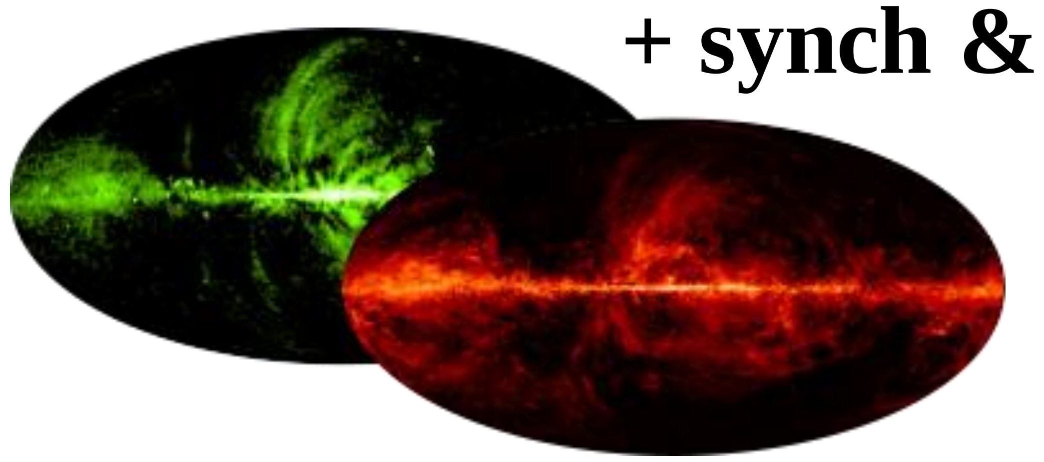

MK technique

α_i, β

β from CMB

Standard component separation

- Parametric SED

CMB

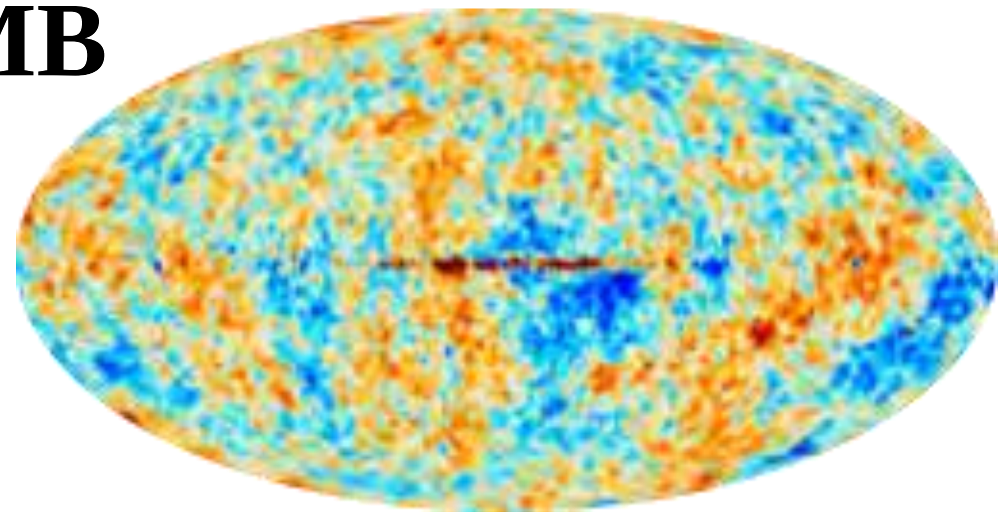

$<\alpha_i> + \beta$ rotated

Harmonic space
D-estimator

Real space
Peak stacking

Modified component separation

- Parametric SED
- $+ \alpha_i$

CMB

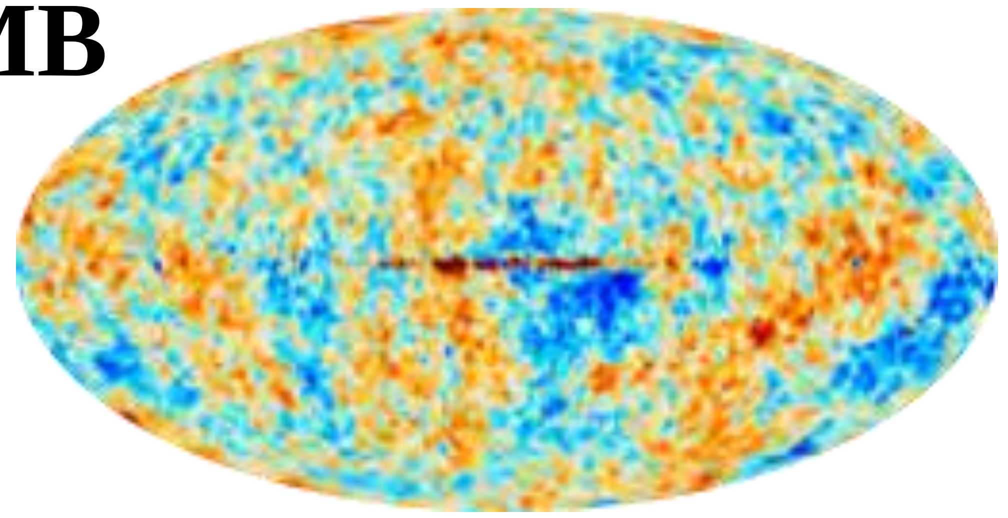

β rotated

Analysis pipelines

Frequency maps

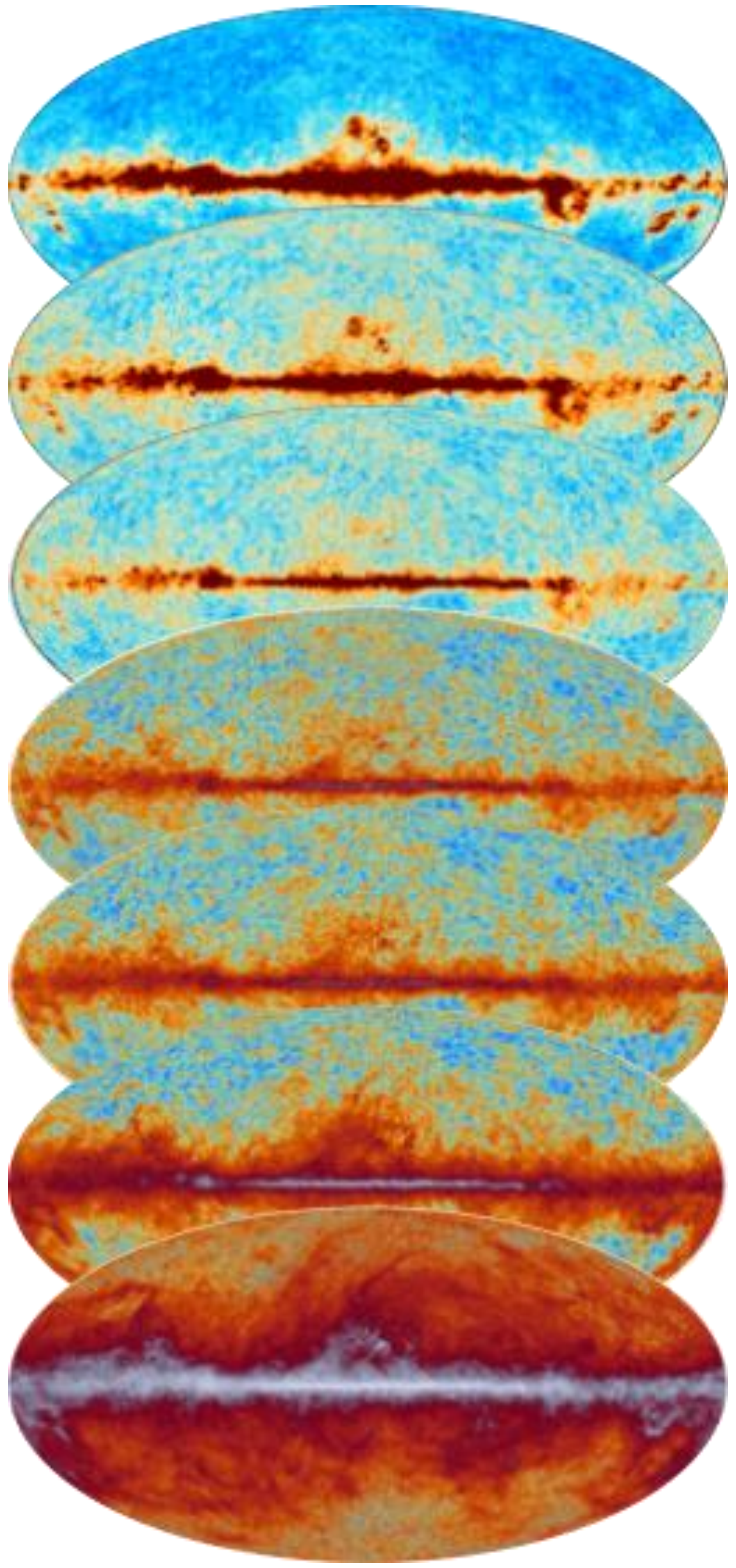

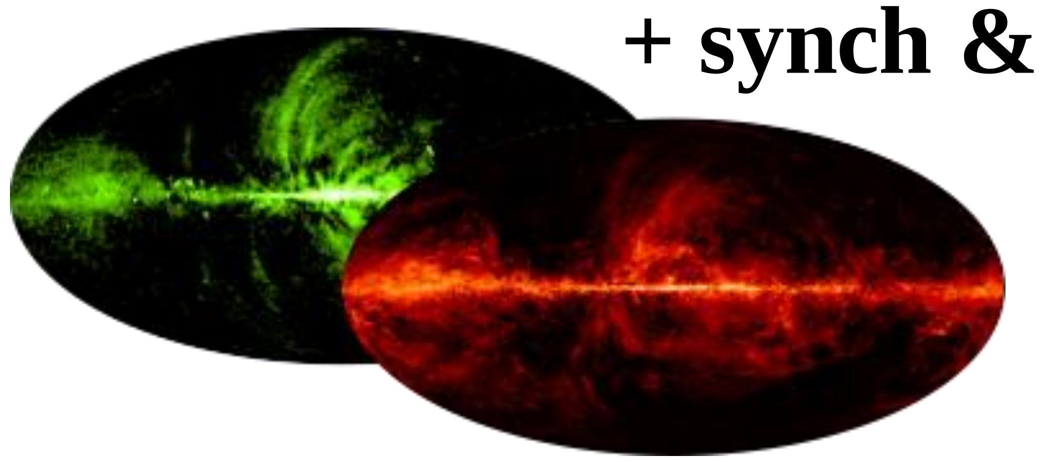

+ synch & dust model

MK technique

Standard component separation

- Parametric SED

Modified component separation

- Parametric SED
- + α_i
- + β + r joint & unbiased estimate of all parameters

α_i, β

CMB

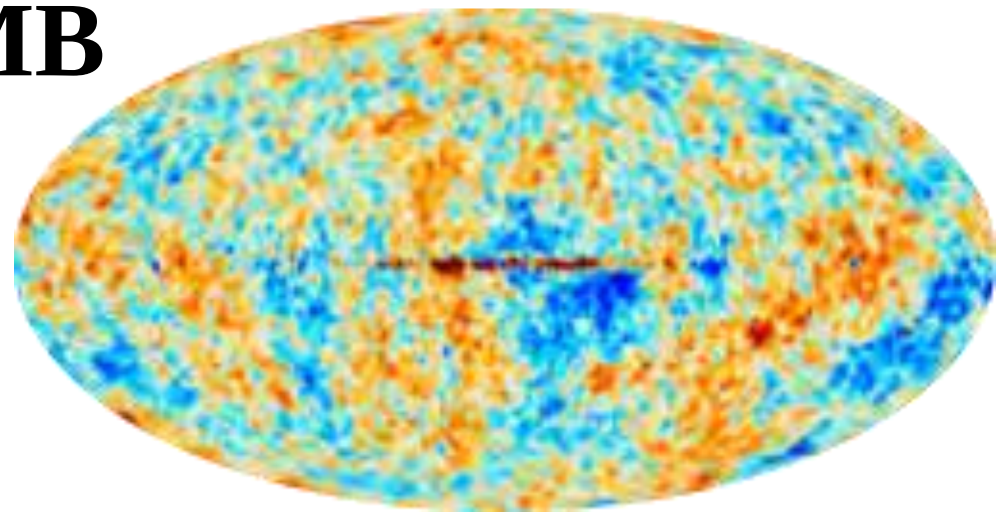

$<\alpha_i> + \beta$ rotated

CMB

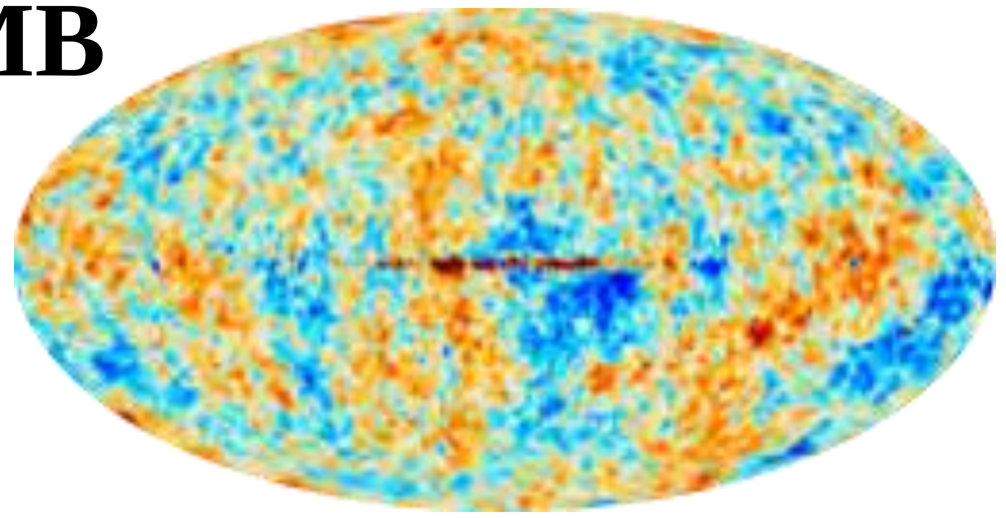

β rotated
Non-rotated

β from CMB

Harmonic space
D-estimator

Real space
Peak stacking

Minami-Komatsu (MK) technique

Considering dust and synchrotron contributions separately

$$C_\ell^{EB,o} = \frac{1}{2}\tan(4\alpha)\left(C_\ell^{EE,o} - C_\ell^{BB,o}\right) + \frac{\sin(4\beta)}{2\cos(4\alpha)}\left(C_\ell^{EE,\mathrm{cmb}} - C_\ell^{BB,\mathrm{cmb}}\right)$$
$$+ \frac{1}{\cos(4\alpha)}\left(C_\ell^{EB,s} + C_\ell^{EB,d} + C_\ell^{E_sB_d} + C_\ell^{E_dB_s}\right)$$

Diego-Palazuelos+ JCAP 2023

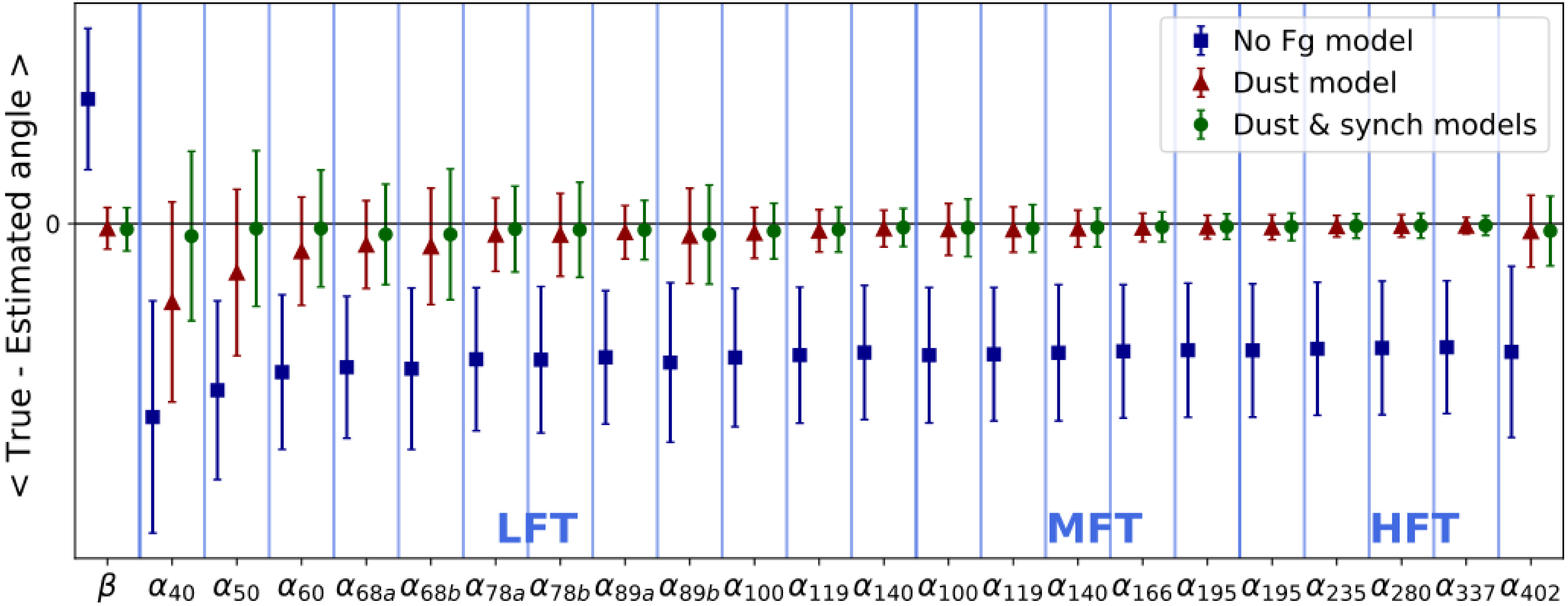

D-estimator

$$D_\ell(\hat{\beta}) = C_\ell^{EB,o} - \frac{1}{2}\tan(4\hat{\beta})\left(C_\ell^{EE,o} - C_\ell^{BB,o}\right)$$

$$\langle D_\ell(\hat{\beta} = \beta)\rangle = 0$$

Find the zeros minimizing

$$\chi^2(\hat{\beta}) = \sum_{\ell\ell'} D_\ell(\hat{\beta}) M^{-1}_{\ell\ell'} D_{\ell'}(\hat{\beta})$$

Build the covariance matrix from simulations to account for foreground debiasing and the extra dispersion caused by α miscalibrations

$$M_{\ell\ell'} = \langle D_\ell D_{\ell'}\rangle$$

Gruppuso+ JCAP 2016

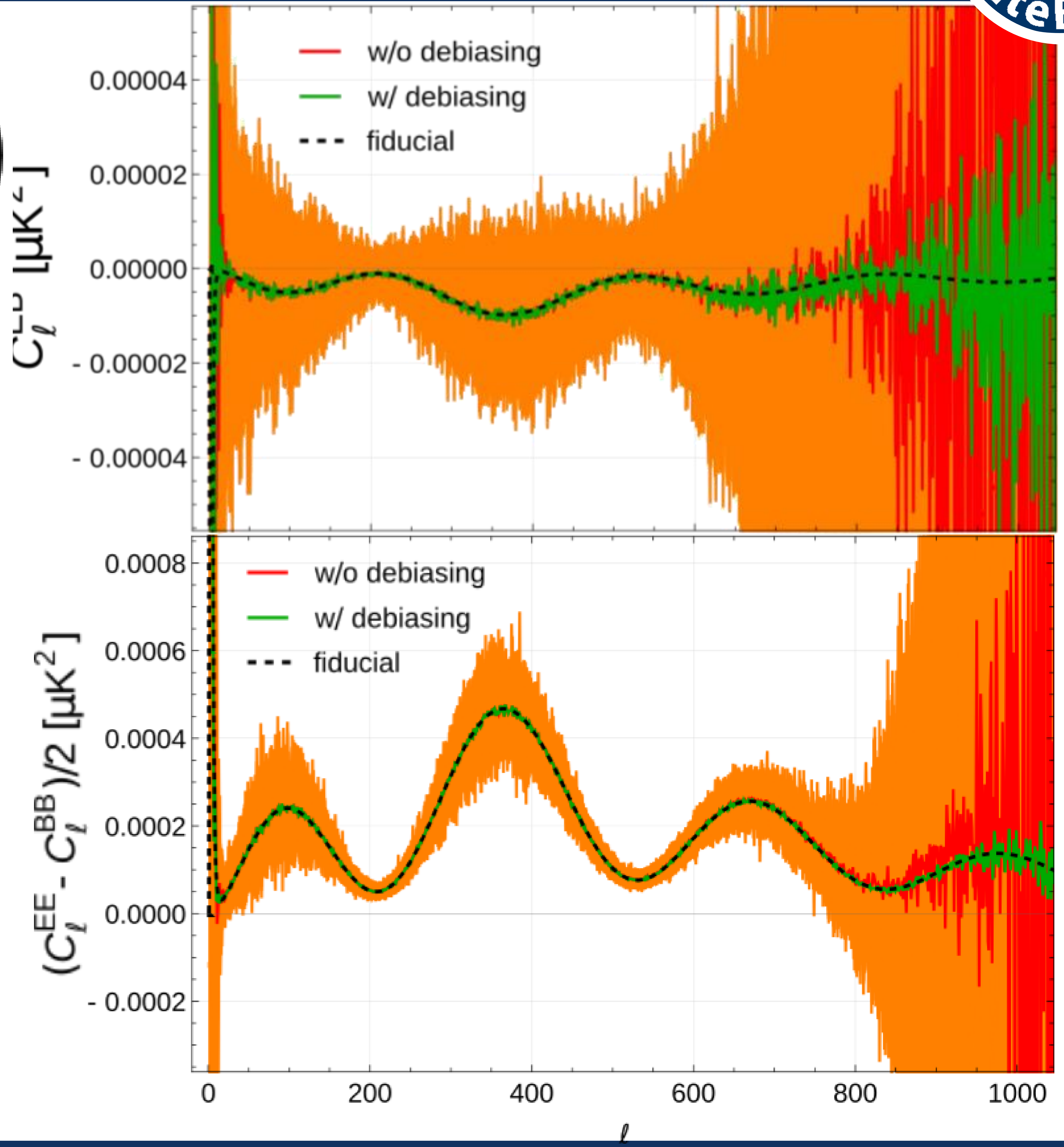

Stacking of peaks

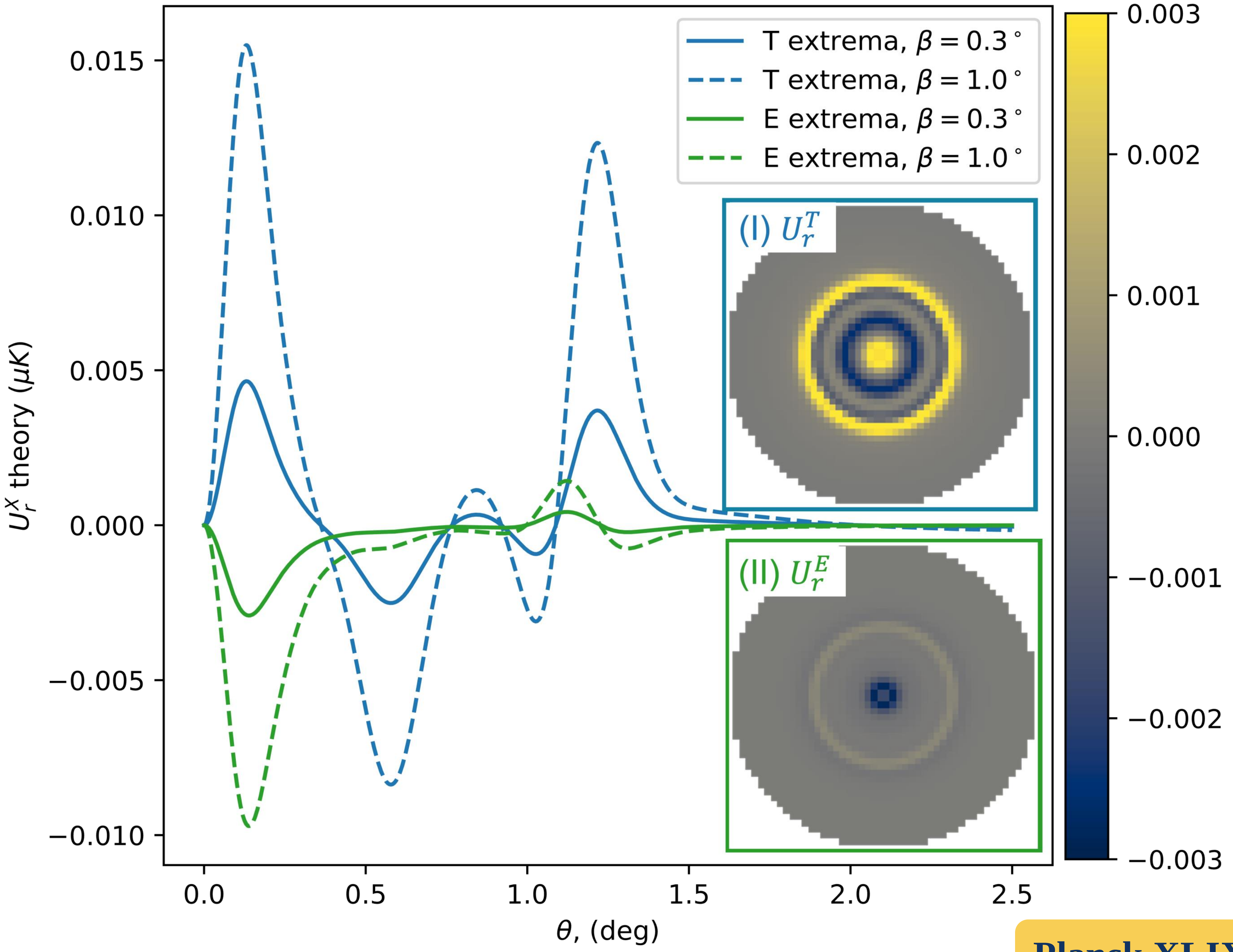

Find local extrema in *T* and *E* anisotropies

Transform the Stokes parameters and stack peaks

$$Q_r(\theta) = -Q(\theta)\cos(2\phi) - U(\theta)\sin(2\phi)$$
$$U_r(\theta) = \quad Q(\theta)\sin(2\phi) - U(\theta)\cos(2\phi)$$

Radial profile around peaks is sensitive to *β*

$$\langle U_r^T \rangle(\theta) = -\sin(2\beta)\int \frac{\ell d\ell}{2\pi} W_\ell^T W_\ell^P J_2(\ell\theta) \times (\bar{b_\nu} + \bar{b_\zeta}\ell^2) C_\ell^{TE}$$

$$\langle U_r^E \rangle(\theta) = -\frac{1}{2}\sin(4\beta)\int \frac{\ell d\ell}{2\pi} W_\ell^E W_\ell^P J_2(\ell\theta) \times (\bar{b_\nu} + \bar{b_\zeta}\ell^2)(C_\ell^{EE} - C_\ell^{BB})$$

Planck XLIX A&A 2016

Component separation + α_i

$$\begin{pmatrix} \boldsymbol{Q}(\boldsymbol{\nu},\theta) \\ \boldsymbol{U}(\boldsymbol{\nu},\theta) \end{pmatrix}_p = \begin{pmatrix} c^{\mathrm{Q}} \\ c^{\mathrm{U}} \end{pmatrix}_p + \begin{pmatrix} a_s^{\mathrm{Q}} \\ a_s^{\mathrm{U}} \end{pmatrix}_p \frac{1}{u(\boldsymbol{\nu})} \left(\frac{\boldsymbol{\nu}}{\nu_s}\right)^{\beta_s} + \begin{pmatrix} a_d^{\mathrm{Q}} \\ a_d^{\mathrm{U}} \end{pmatrix}_p \frac{1}{u(\boldsymbol{\nu})} \left(\frac{\boldsymbol{\nu}}{\nu_d}\right)^{\beta_d - 2} \frac{B(\boldsymbol{\nu}, T_d)}{B(\nu_d, T_d)}$$

$$\begin{pmatrix} \boldsymbol{Q}^{\mathrm{o}}(\boldsymbol{\nu},\boldsymbol{\alpha},\theta) \\ \boldsymbol{U}^{\mathrm{o}}(\boldsymbol{\nu},\boldsymbol{\alpha},\theta) \end{pmatrix}_p = \begin{pmatrix} \cos(2\boldsymbol{\alpha}) & -\sin(2\boldsymbol{\alpha}) \\ \sin(2\boldsymbol{\alpha}) & \cos(2\boldsymbol{\alpha}) \end{pmatrix} \begin{pmatrix} \boldsymbol{Q}(\boldsymbol{\nu},\theta) \\ \boldsymbol{U}(\boldsymbol{\nu},\theta) \end{pmatrix}_p$$

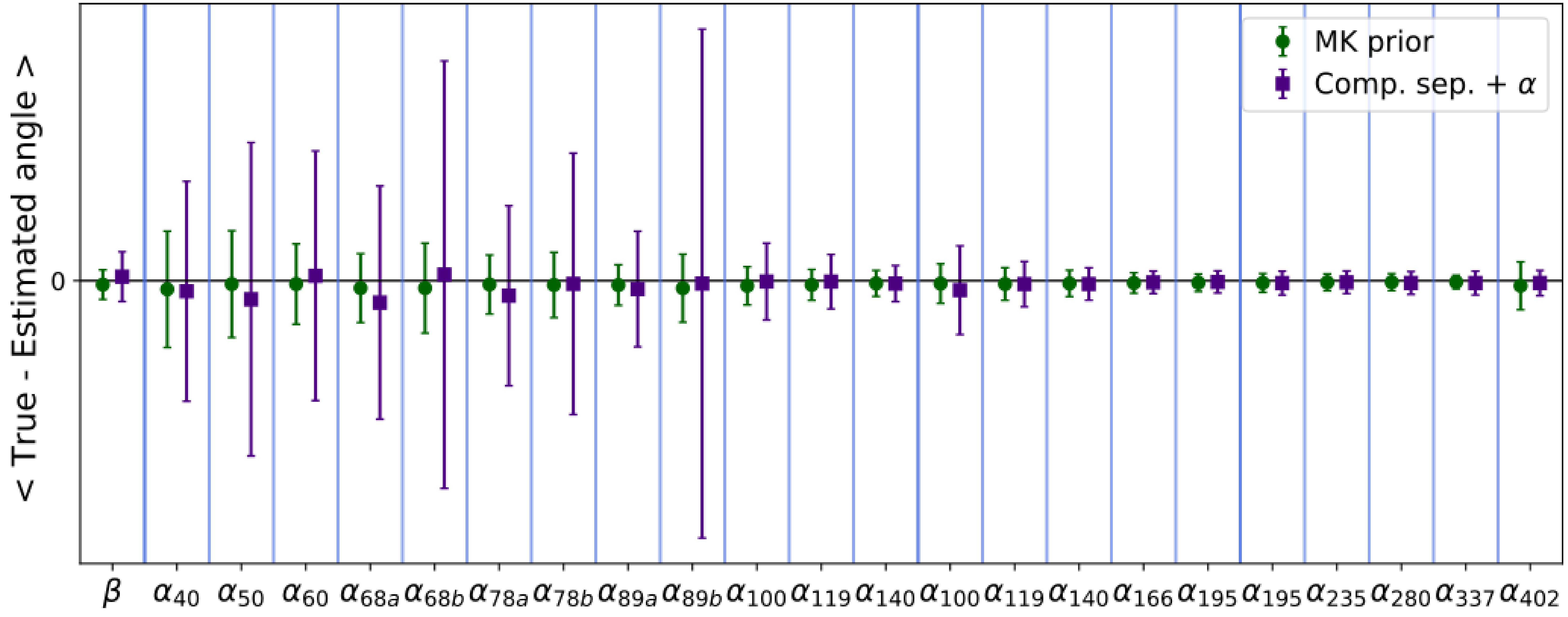

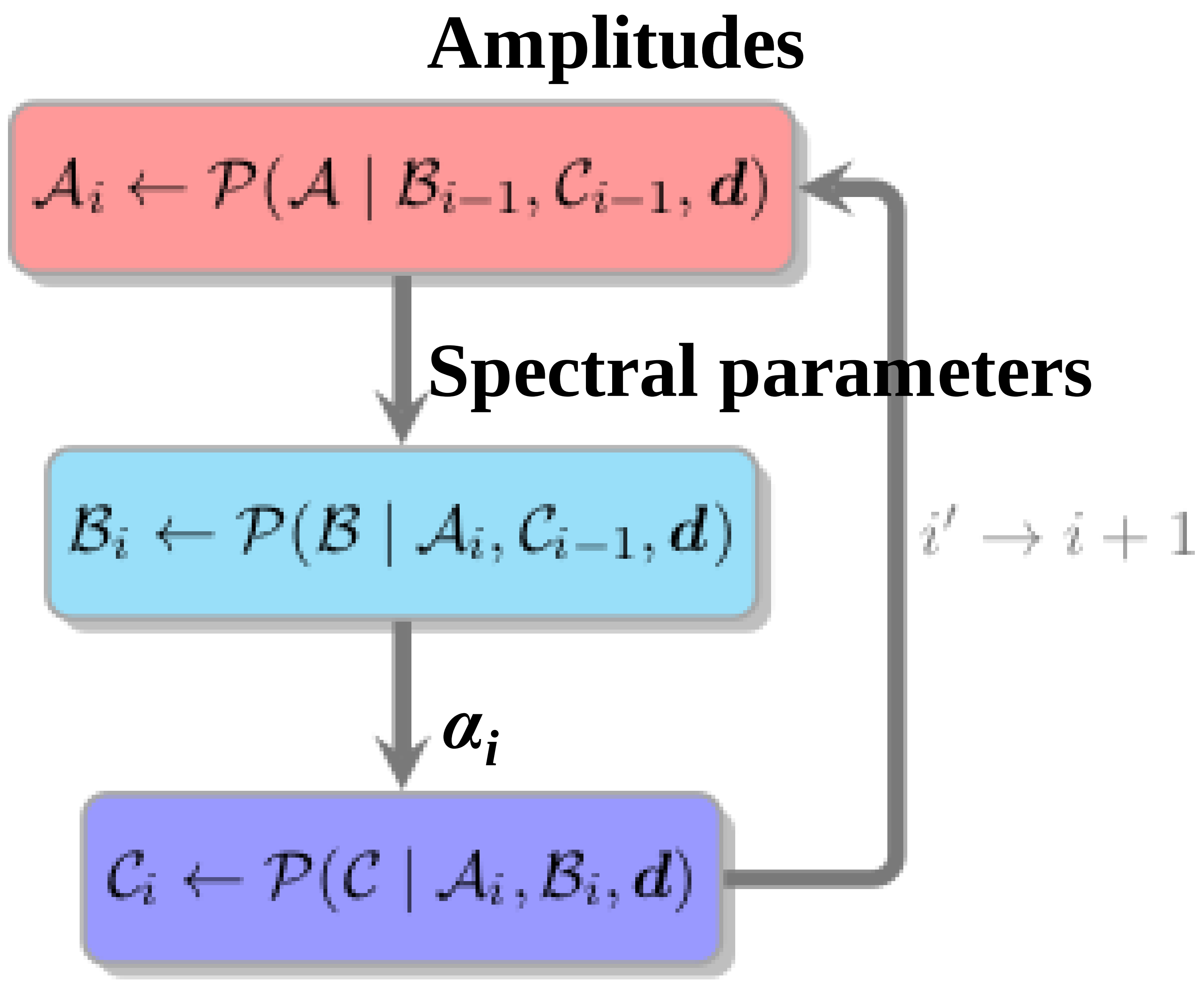

Gaussian priors on spectral parameters
MK result as prior on α_i

de la Hoz+ JCAP 2022

Component separation + $\alpha_i + \beta + r$

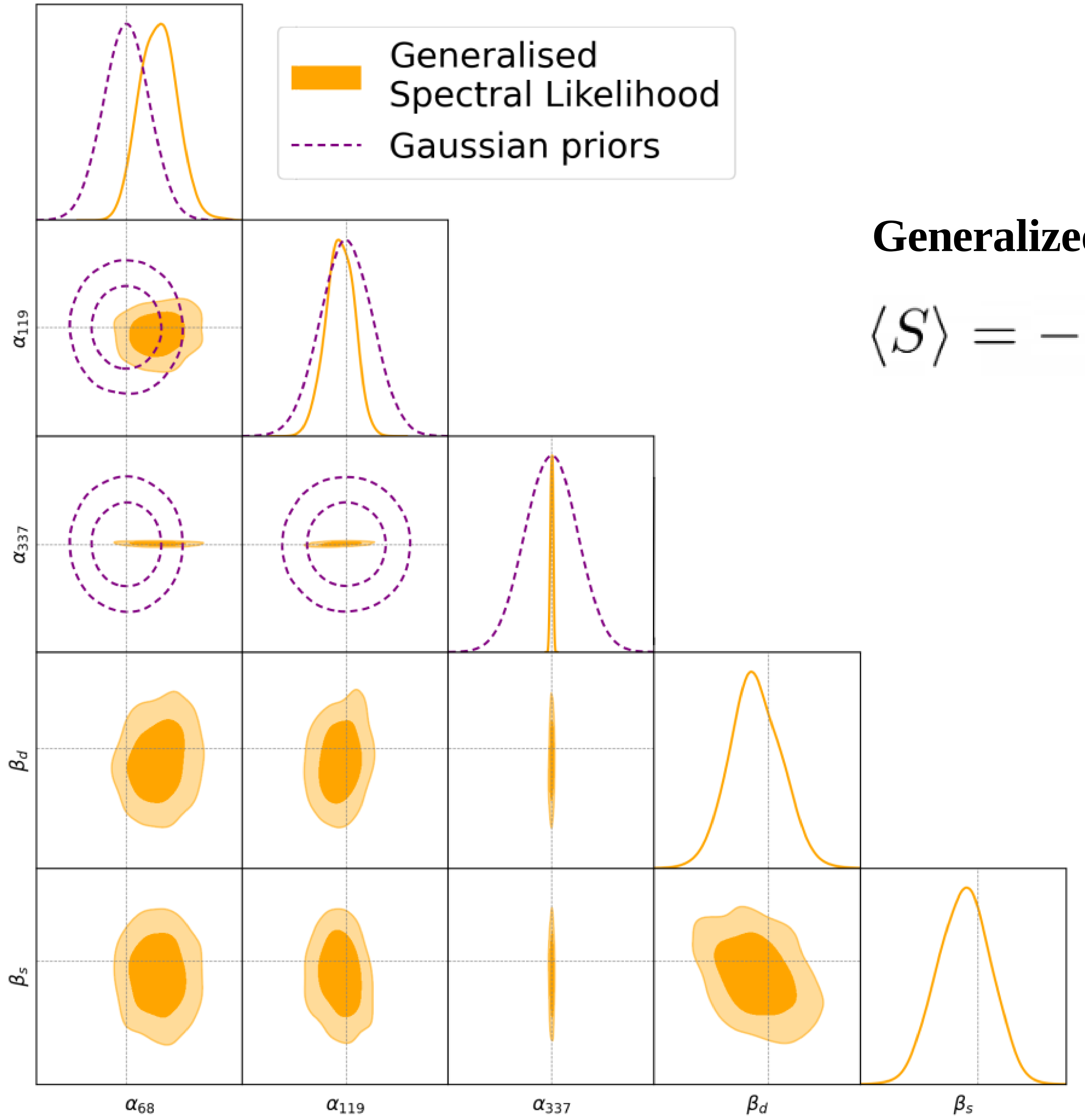

Generalized spectral likelihood

$$\langle S \rangle = -2 \sum \mathrm{tr}\left(\boldsymbol{N}_p^{-1} \boldsymbol{\Lambda}_p (\boldsymbol{\Lambda}_p^t \boldsymbol{N}_p^{-1} \boldsymbol{\Lambda}_p)^{-1} \boldsymbol{\Lambda}_p^t \boldsymbol{N}_p^{-1} \langle \boldsymbol{d}_p \boldsymbol{d}_p^t \rangle \right)$$

Stompor+ MNRAS 2009
Vergès+ PRD 2021

Spectral parameters

$$\boldsymbol{d} = \underbrace{\boldsymbol{X}\,\boldsymbol{A}}_{\boldsymbol{\Lambda}}\,\underbrace{\boldsymbol{\mathcal{B}}\,\boldsymbol{c}}_{\boldsymbol{s}} + \boldsymbol{n}$$

Birefringence

Instrument miscalibration

Component separation + $\alpha_i + \beta + r$

Jost+ PRD 2023

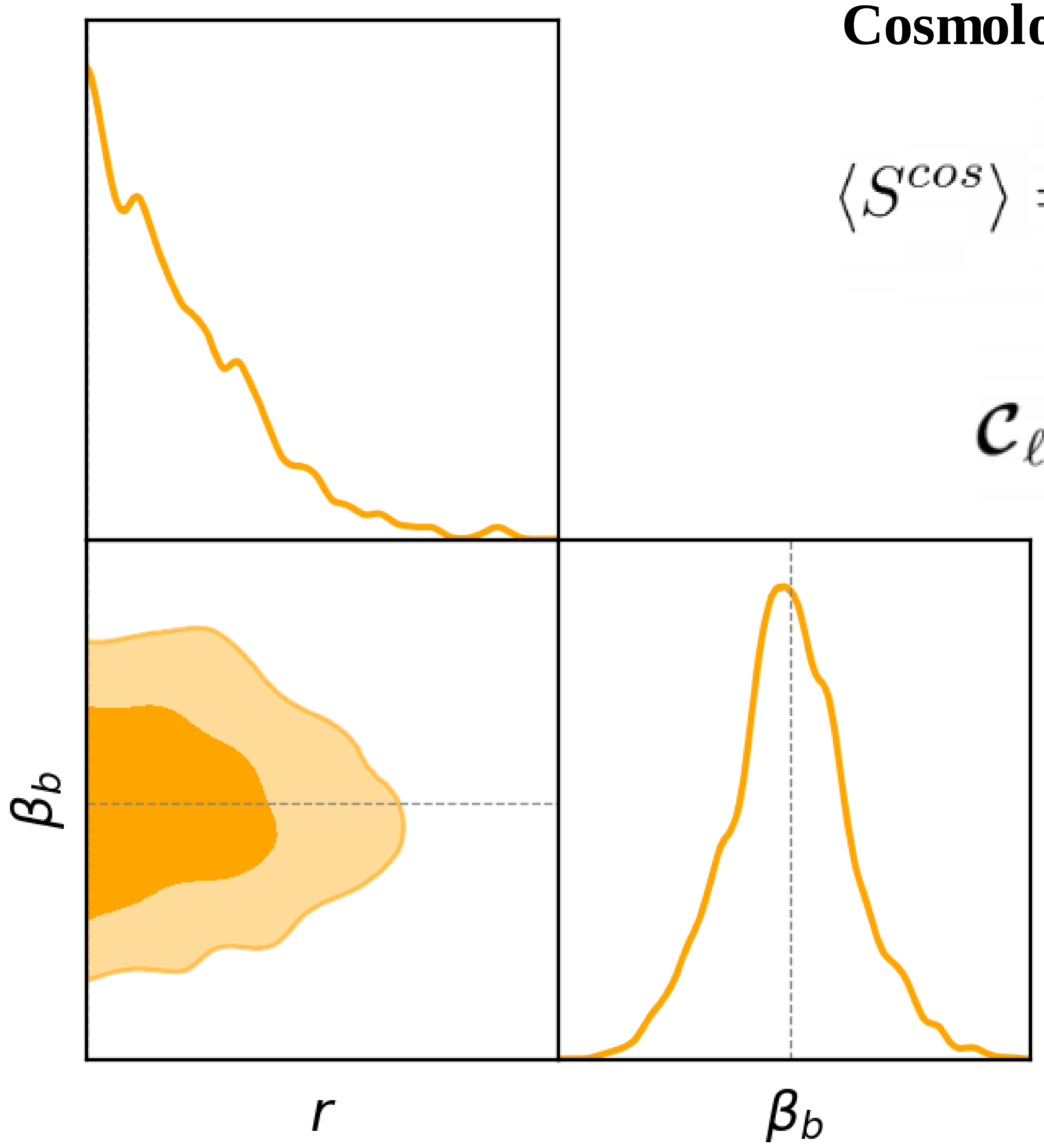

Cosmological likelihood

Output of spectral likelihood

$$\langle S^{cos} \rangle = f_{sky} \sum_{\ell=\ell_{min}}^{\ell_{max}} \frac{(2\ell+1)}{2} \left(Tr(\boldsymbol{C}_\ell^{-1} \boldsymbol{E}_\ell) + \ln(\det(\boldsymbol{C}_\ell)) \right)$$

$$\boldsymbol{\mathcal{C}}_\ell(r, \beta_b) \equiv$$

$$\boldsymbol{\mathcal{R}}(\beta_b) \begin{pmatrix} C_\ell^{EE,\mathrm{p}} & 0 \\ 0 & rC_\ell^{BB,\mathrm{p}} + A_L C_\ell^{BB,\mathrm{lens}} \end{pmatrix} \boldsymbol{\mathcal{R}}^{-1}(\beta_b) + C_\ell^{\mathrm{noise}}$$

Gaussian priors on spectral parameters
External priors from an artificial or astrophysical calibration source on some frequency channels

Performance across pipelines

Phase1

CMB (β=0)
+ noise
+ simple foregrounds (s0d0)

Phase 2

CMB (β=0)
+ noise
+ complex foregrounds (s1d1)

Phase 3

CMB (β=0)
+ noise
+ complex foregrounds (s1d1)
+ systematics ($\alpha_i \neq 0$)

Phase 4

CMB ($\beta \neq 0$)
+ noise
+ complex foregrounds (s1d1)
+ systematics ($\alpha_i \neq 0$)

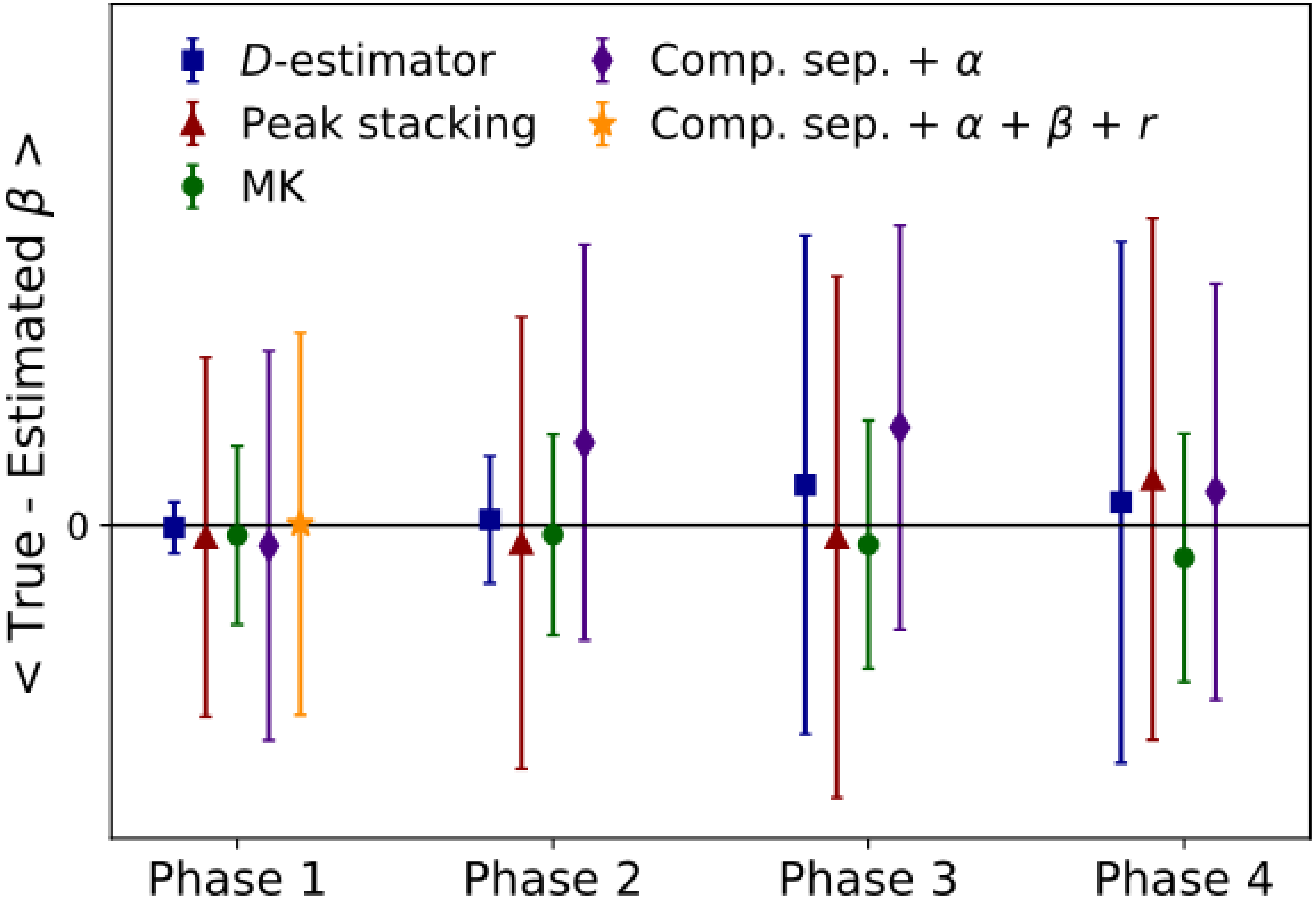

Take-home message

LiteBIRD will provide the perfect venue to confirm the current hints of $\beta \approx 0.3$ found in *Planck* and WMAP data

We are developing different complementary analysis pipelines

Robust analysis

Internally assess the impact of instrumental miscalibrations and Galactic foregrounds on our measurements

Analysis pipelines have succesfully adapted to overcome the different levels of complexity

Future work

Continue exploring more complex foregrounds and additional sources of systematics

Keep an eye on the arXiv for the full forecast soon!

LiteBIRD

APC
ASI
Berkeley UNIVERSITY OF CALIFORNIA
BERKELEY LAB
UNIVERSITÀ DEGLI STUDI DI MILANO BICOCCA
CARDIFF UNIVERSITY PRIFYSGOL CAERDYDD
cea
Centre Pierre Binétruy CNRS • Berkeley
cnes
cnrs
CSA ASC Canada

CSIC CONSEJO SUPERIOR DE INVESTIGACIONES CIENTÍFICAS
CSL CENTRE SPATIAL DE LIÈGE
ENS | PSL
erc European Research Council Established by the European Commission
EXCELENCIA MARÍA DE MAEZTU
EXCELENCIA SEVERO OCHOA
FAU FRIEDRICH-ALEXANDER UNIVERSITÄT ERLANGEN-NÜRNBERG
Forskningsrådet The Research Council of Norway

GOBIERNO DE ESPAÑA MINISTERIO DE CIENCIA E INNOVACIÓN
NASA Goddard Space Flight Center
GSSI GRAN SASSO SCIENCE INSTITUTE
INSTITUTO DE ASTROFISICA DE CANARIAS IAC
IAP
IAS Orsay
IFCA Instituto de Física de Cantabria

ifpU
IJCLab Irène Joliot-Curie Laboratoire de Physique des 2 Infinis
INFN
INAF ISTITUTO NAZIONALE DI ASTROFISICA
IPMU INSTITUTE FOR THE PHYSICS AND MATHEMATICS OF THE UNIVERSE
IPNS 素粒子原子核研究所 Institute of Particle and Nuclear Studies

irap astrophysique & planétologie
JAXA
KEK
KIPAC
KMI Kobayashi-Maskawa Institute Nagoya University
LMU USM
LPSC GRENOBLE | MODANE

MAX-PLANCK-INSTITUT FÜR ASTROPHYSIK
McGill
名古屋大学 NAGOYA UNIVERSITY
NATIONAL INSTITUTE OF TECHNOLOGY KAGAWA COLLEGE 香川高専
NÉEL institut
NIST
Norwegian Directorate for Higher Education and Skills

岡山大学 OKAYAMA UNIVERSITY
QUP International Center for Quantum-field Measurement Systems for Studies of the Universe and Particles
POLITÉCNICA | idr
PRINCETON UNIVERSITY
SAPIENZA UNIVERSITÀ DI ROMA
SISSA
SORBONNE UNIVERSITÉ
SSDC SPACE SCIENCE DATA CENTER
LELAND STANFORD JUNIOR UNIVERSITY 1891

Stockholm University
公立諏訪東京理科大学 Suwa University of Science
TOR VERGATA UNIVERSITÀ DEGLI STUDI DI ROMA
UCL
UBC THE UNIVERSITY OF BRITISH COLUMBIA
UC UNIVERSIDAD DE CANTABRIA
University of Colorado Boulder
UKRI Science and Technology Facilities Council
ULB UNIVERSITÉ LIBRE DE BRUXELLES

Universidad de La Laguna
MANCHESTER 1824 The University of Manchester
UiO University of Oslo
UNIVERSITÀ DI PISA 1343
Università degli Studi di Ferrara
UNIVERSITÀ DEGLI STUDI DI MILANO
UNIVERSITÀ DEGLI STUDI DI PADOVA
THE UNIVERSITY OF TOKYO
UNIVERSITY OF TORONTO

Component separation + α + β + r

3rd) Instrument miscalibration

$$\boldsymbol{X}(\{\alpha_1, ..., \alpha_{n_f}\}) = \begin{pmatrix} \cos(2\alpha_1) & \sin(2\alpha_1) & & & 0 \\ -\sin(2\alpha_1) & \cos(2\alpha_1) & & & \\ & & \ddots & & \\ & & & \cos(2\alpha_{n_f}) & \sin(2\alpha_{n_f}) \\ 0 & & & -\sin(2\alpha_{n_f}) & \cos(2\alpha_{n_f}) \end{pmatrix}$$

$$\boldsymbol{d} = \underbrace{\boldsymbol{X}\,\boldsymbol{A}}_{\boldsymbol{\Lambda}}\,\underbrace{\boldsymbol{\mathcal{B}}\,\boldsymbol{c}}_{\boldsymbol{s}} + \boldsymbol{n}$$

2nd) Mixing matrix

$$\boldsymbol{A}(\{\beta_{fg}\}) = \begin{pmatrix} 1 & 0 & A_1^d & 0 & A_1^s & 0 \\ 0 & 1 & 0 & A_1^d & 0 & A_1^s \\ \vdots & \vdots & \vdots & \vdots & \vdots & \vdots \\ 1 & 0 & A_n^d & 0 & A_n^s & 0 \\ 0 & 1 & 0 & A_n^d & 0 & A_n^s \end{pmatrix}$$

CMB Dust Synch

1st) Birefringent rotation of CMB

$$\boldsymbol{\mathcal{B}}(\{\beta_b\}) = \begin{pmatrix} \cos(2\beta_b) & \sin(2\beta_b) & 0 & 0 & 0 & 0 \\ -\sin(2\beta_b) & \cos(2\beta_b) & 0 & 0 & 0 & 0 \\ 0 & 0 & 1 & 0 & 0 & 0 \\ 0 & 0 & 0 & 1 & 0 & 0 \\ 0 & 0 & 0 & 0 & 1 & 0 \\ 0 & 0 & 0 & 0 & 0 & 1 \end{pmatrix}$$

Component separation + $\alpha_i + \beta + r$

Instrument miscalibration → X, **Spectral parameters** → A, **Birefringence** → $\mathcal{B}$

$$\boldsymbol{d} = \underbrace{\boldsymbol{X}\,\boldsymbol{A}}_{\boldsymbol{\Lambda}}\,\underbrace{\boldsymbol{\mathcal{B}}\,\boldsymbol{c}}_{\boldsymbol{s}} + \boldsymbol{n}$$

Generalized spectral likelihood

$$\langle S \rangle = -2 \sum \mathrm{tr}\left(\boldsymbol{N}_p^{-1}\boldsymbol{\Lambda}_p(\boldsymbol{\Lambda}_p^t\boldsymbol{N}_p^{-1}\boldsymbol{\Lambda}_p)^{-1}\boldsymbol{\Lambda}_p^t\boldsymbol{N}_p^{-1}\langle \boldsymbol{d}_p\boldsymbol{d}_p^t\rangle\right)$$

Cosmological likelihood — **Output of spectral likelihood** ($\boldsymbol{E}_\ell$)

$$\langle S^{cos}\rangle = f_{sky}\sum_{\ell=\ell_{min}}^{\ell_{max}}\frac{(2\ell+1)}{2}\left(Tr(\boldsymbol{C}_\ell^{-1}\boldsymbol{E}_\ell) + \ln(\det(\boldsymbol{C}_\ell))\right)$$

$$\boldsymbol{\mathcal{C}}_\ell(r,\beta_b) \equiv \boldsymbol{\mathcal{R}}(\beta_b)\begin{pmatrix} C_\ell^{EE,\mathrm{p}} & 0 \\ 0 & rC_\ell^{BB,\mathrm{p}} + A_L C_\ell^{BB,\mathrm{lens}}\end{pmatrix}\boldsymbol{\mathcal{R}}^{-1}(\beta_b) + C_\ell^{\mathrm{noise}}$$

Gaussian priors on spectral parameters

External calibration priors from an artificial or astrophysical calibration source on some frequency channels

LiteBIRD Joint Study Group

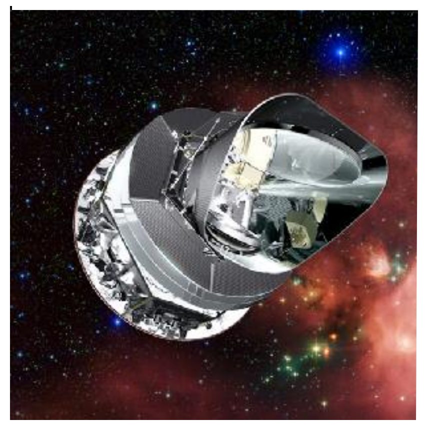



Over 300 researchers from **Japan**, **North America** and **Europe**

Team experience in CMB experiments, X-ray satellites and other large projects (ALMA, HEP experiments, …)

LiteBIRD Global F2F meeting
December 11-13, 2019 at MPE

LiteBIRD other science outcomes

- The mission specifications are driven by the required sensitivity on *r*
- Meeting those sensitivity requirements would allow to address other important scientific topics, such as:

1. Characterize the *B*-mode power spectrum and search for source source fields (e.g. scale-invariance, non-Gaussianity, parity violation, …)
2. Power spectrum features in polarization
   - Large-scale ***E*-modes**
   - **Reionization** (improve $\sigma(\tau)$ by a factor of 3)
   - **Neutrino mass** ($\sigma(\sum m_\nu) = 15$ meV)
3. Constraints on **cosmic birefringence**
4. **SZ effect** (thermal, diffuse, relativistic corrections)
5. Elucidating **anomalies**
6. **Galactic science**
   - Characterizing the foreground SED
   - Large-scale Galactic magnetic field
   - Models of dust polarization

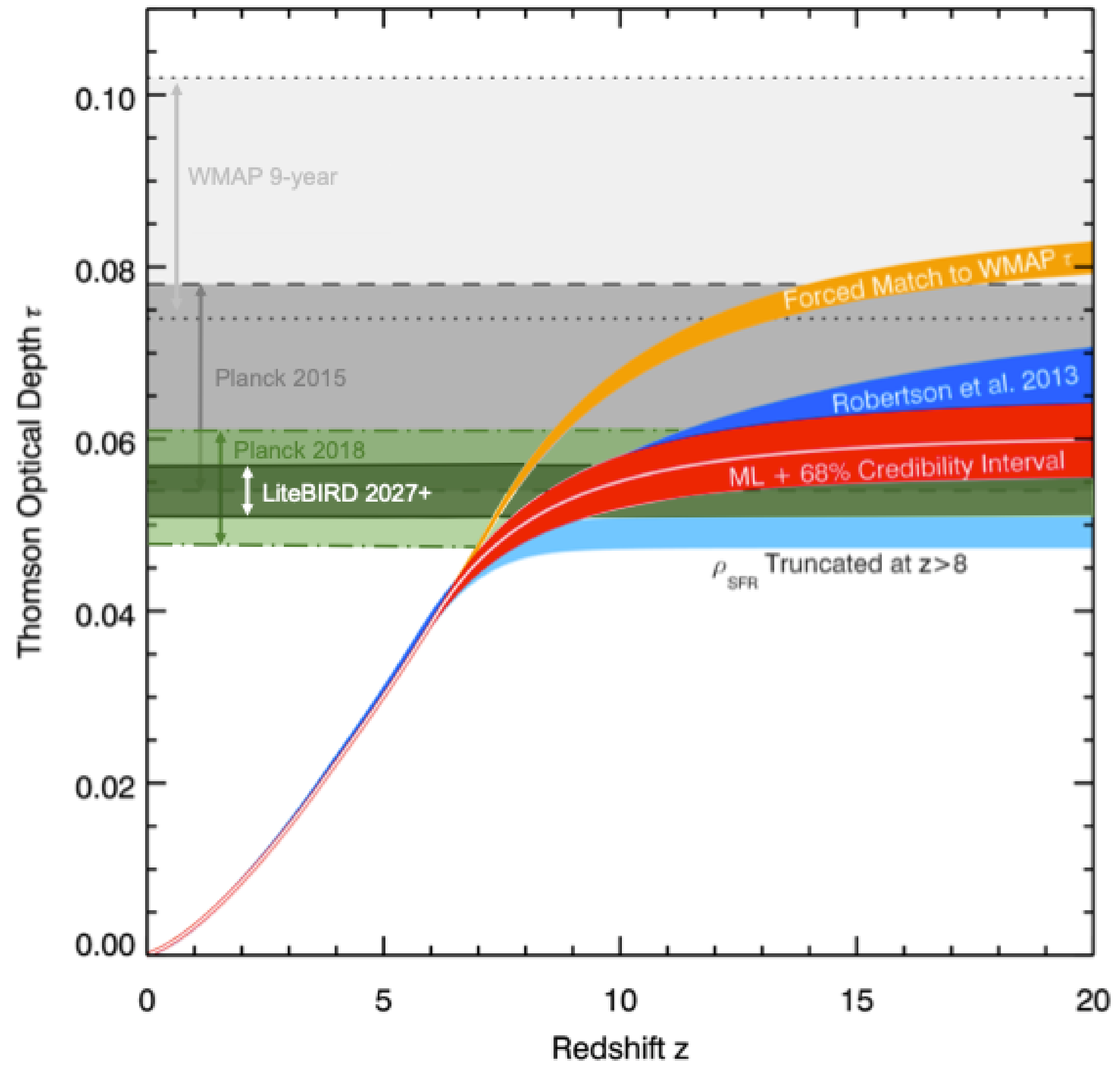

adapted from Robertson+2015

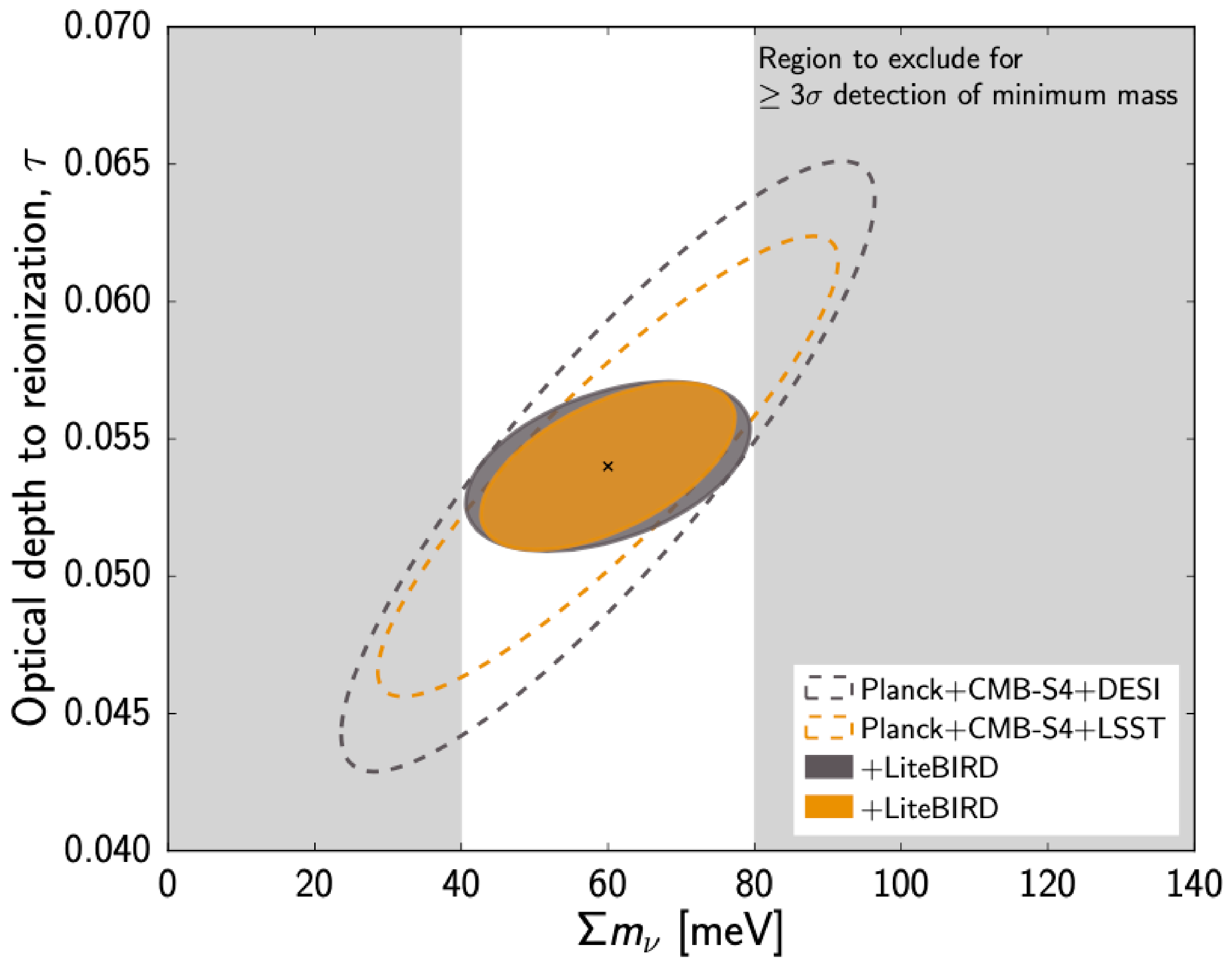

adapted from Calabrese+2017

LiteBIRD scanning strategy

- 3-year survey, Sun-Earth L2 Lissajous orbit
- Precession angle: α = 45°
- Spin angle: β = 50°

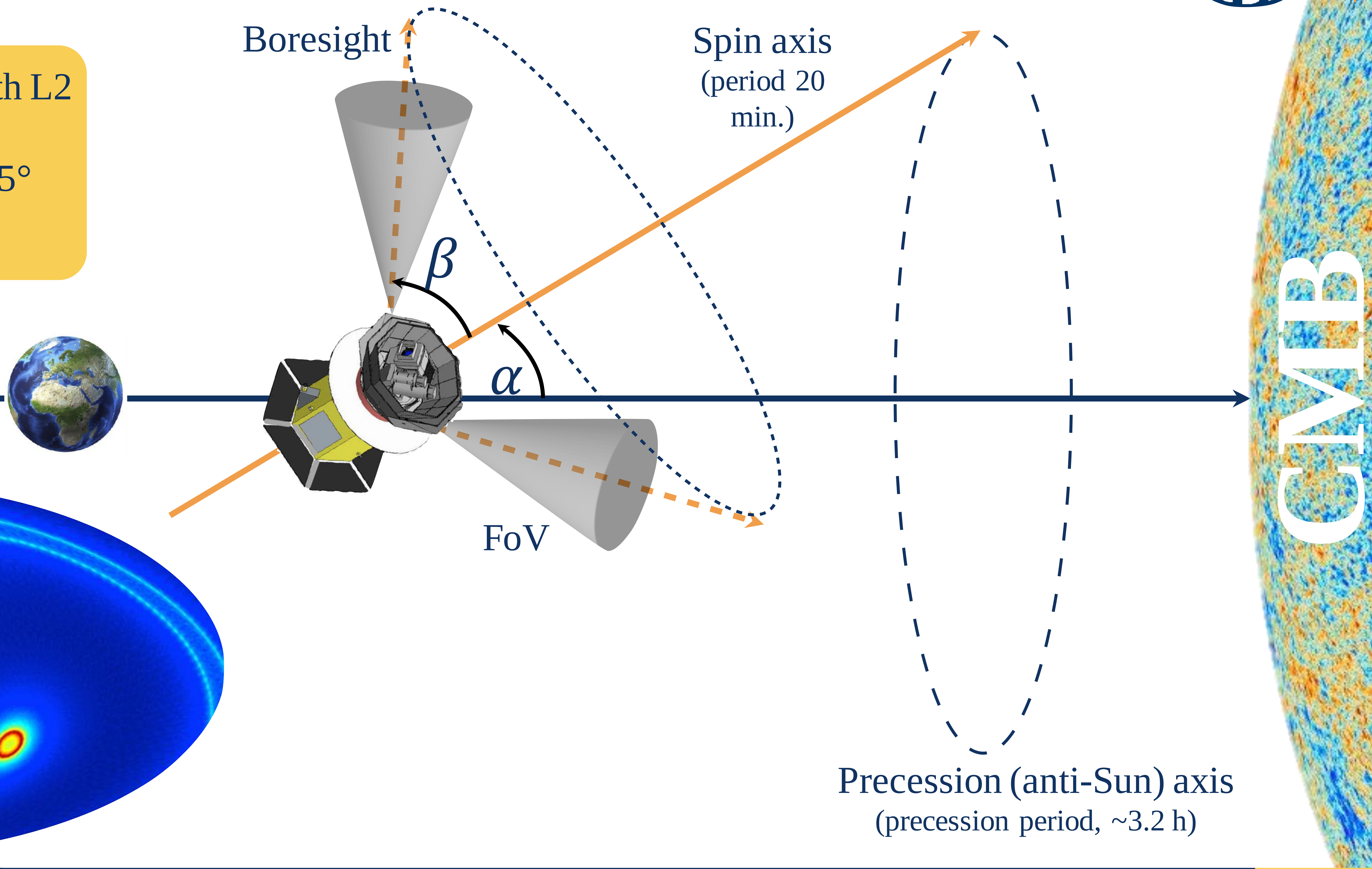

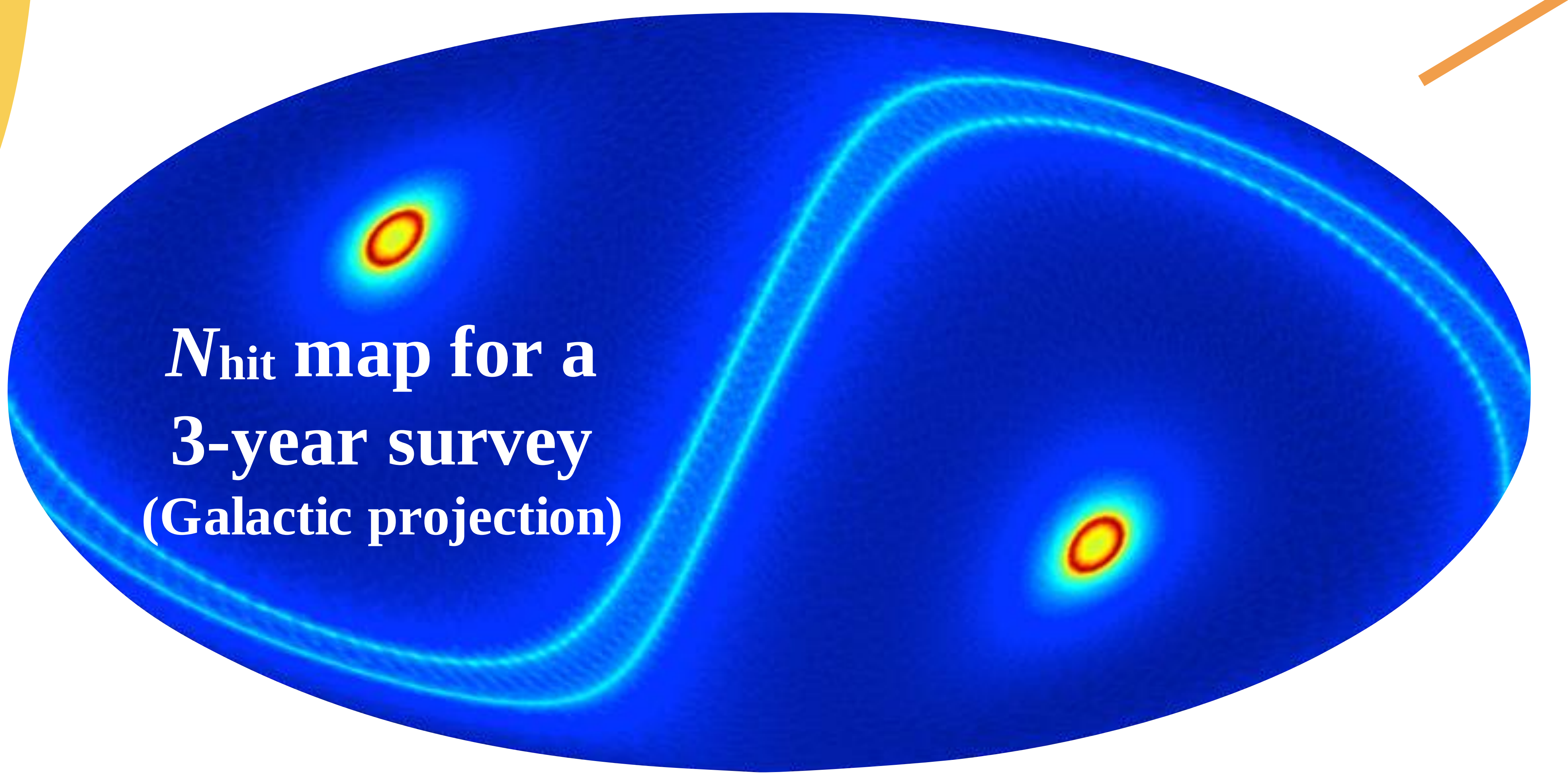

Low Frequency Telescope (LFT)

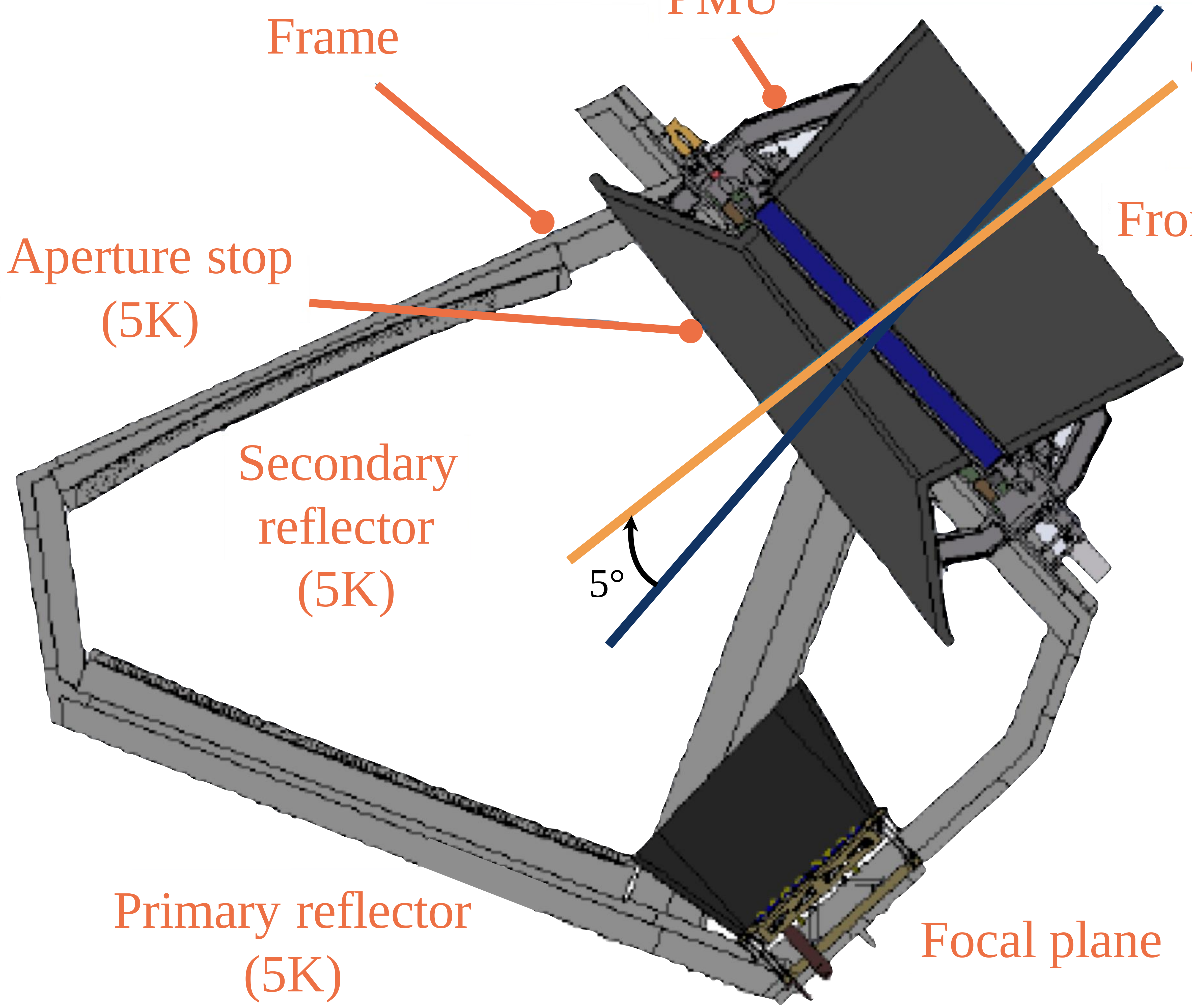

- Polarization Modulation Unit (PMU) as the first sky-side optical element
- **Crossed-Dragone** design
  - Mirrors and aperture stop at **5 K**
  - Made of aluminium
- Field of view: **18°╳9°**
- Strehl ratio > 0.95 (@ 140 GHz)
- Aperture diameter: **400 mm**
- Frequency range: **40-140 GHz**
- Angular resolution: **70-24 arcmin**
- F#3.0 & cross angle of 90°
- Cross-polarization < **-30 dB**
- Rotation of the polarization angle across the FoV < ±1.5°
- Weight < 200 kg

📖 Sekimoto+ SPIE 2020

Middle-High Frequency Telescopes (MFT/HFT)

Montier+ SPIE 2020

Lamagna+ SPIE 2020

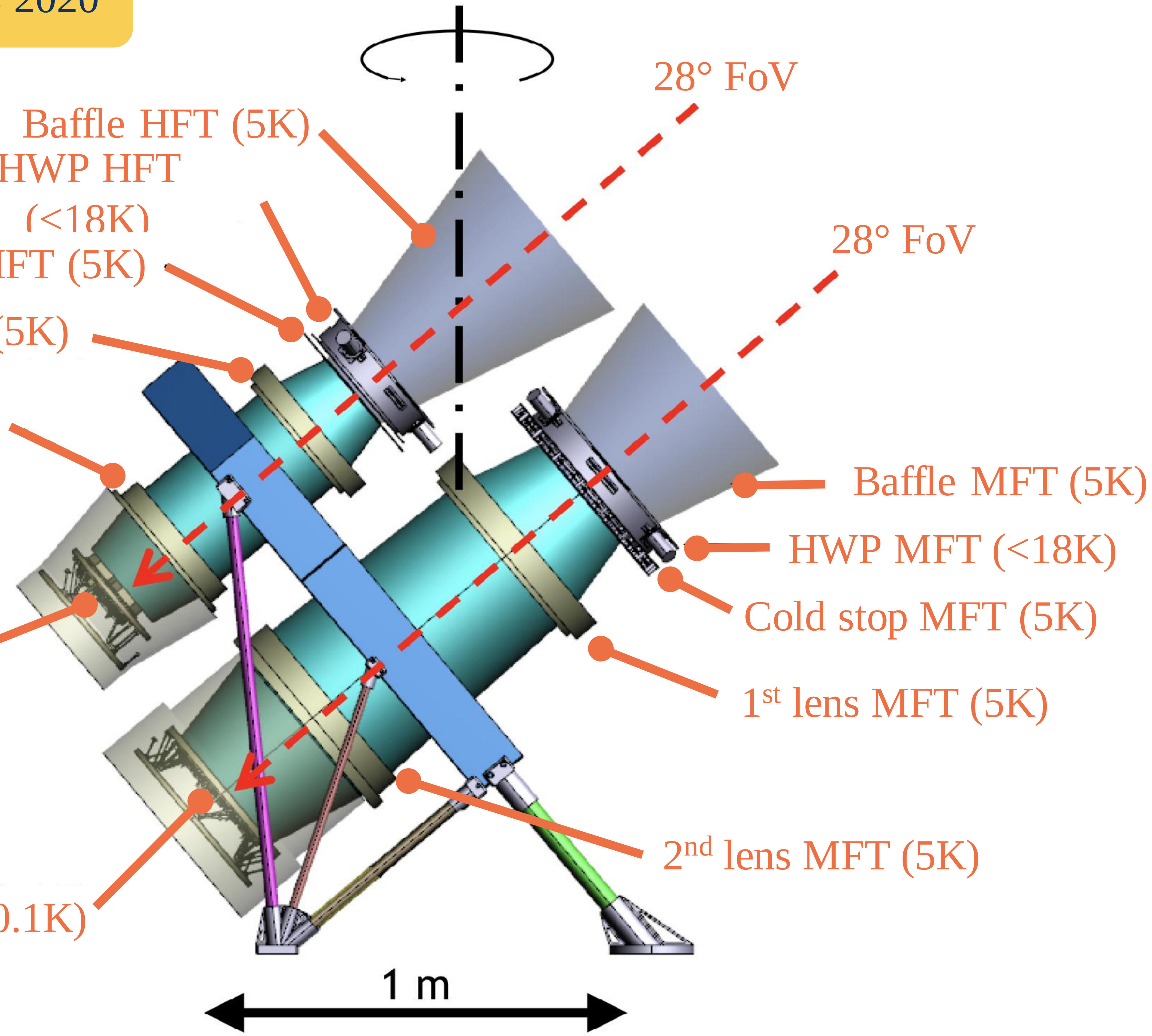

- Refractive optics
- Each telescope has PMU with a half-wave-plate (HWP)
- Optics at **5 K**
- Field of view: **28°**
- Simple and high heritage from ground experiments
- Compact (mass & volume)
- Simplified design for filtering scheme
- PP lenses + ARC
- Weight 180 kg

	MFT	HFT
ν (GHz)	**100-195**	**195-402**
Ap. diameter (mm)	**300**	**200**
Ang. res. (arcmin)	**38-28**	**29-18**

Focal plane configuration

- Transition-Edge Sensor (TES) arrays
- Multichroic detectors
- Number of sensors: 4508
- 15 bands including overlap between instruments

LFT

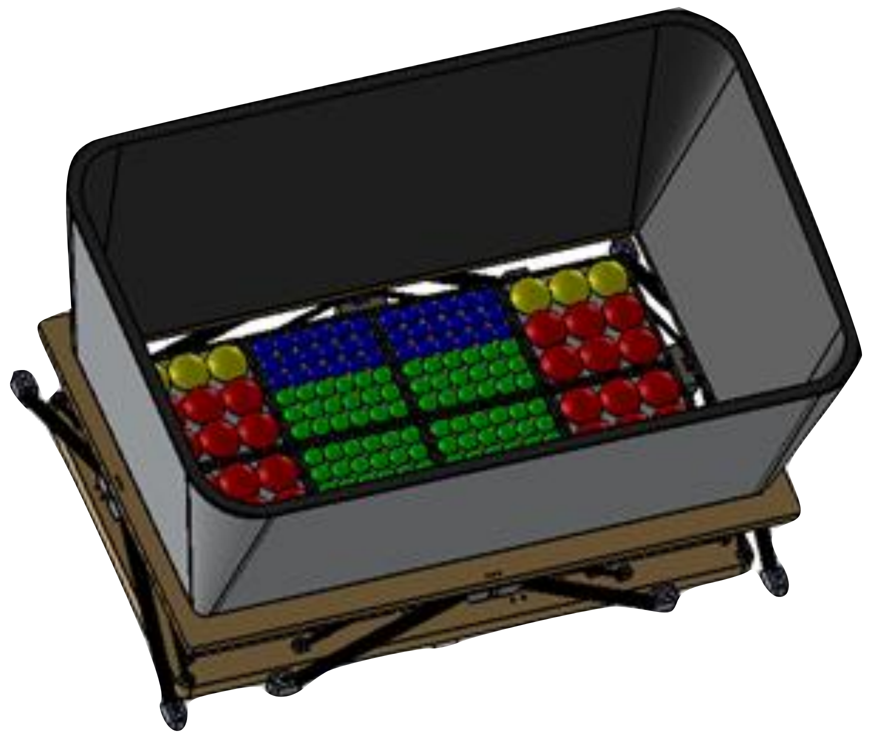

MFT

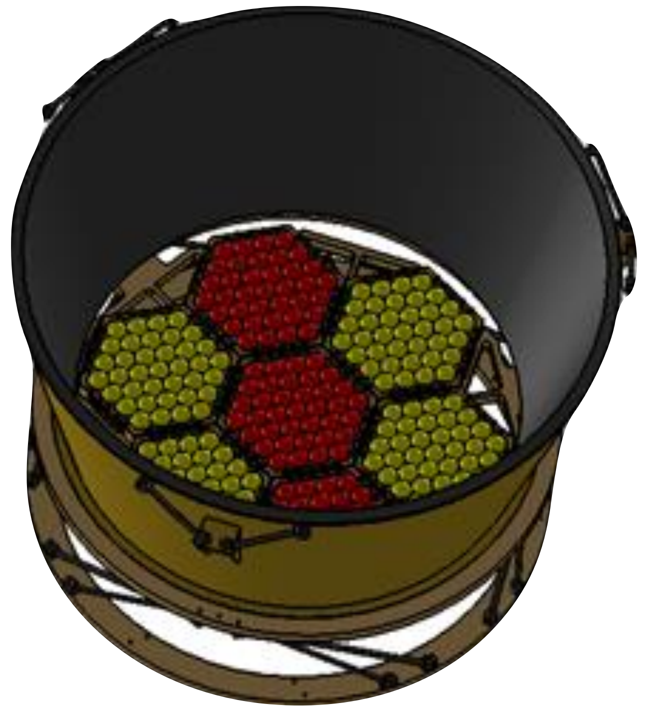

HFT

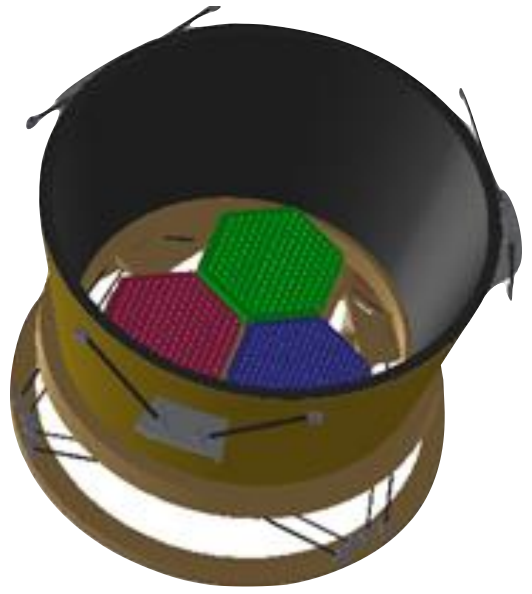

Rule of thumb:
1000 detectors in space = 100 000 detectors on ground

Lensed coupled detectors
Lenslets

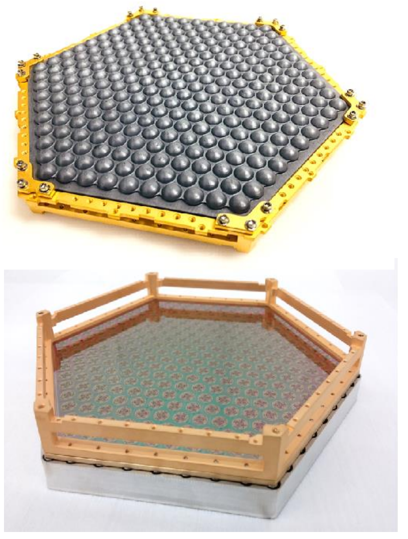

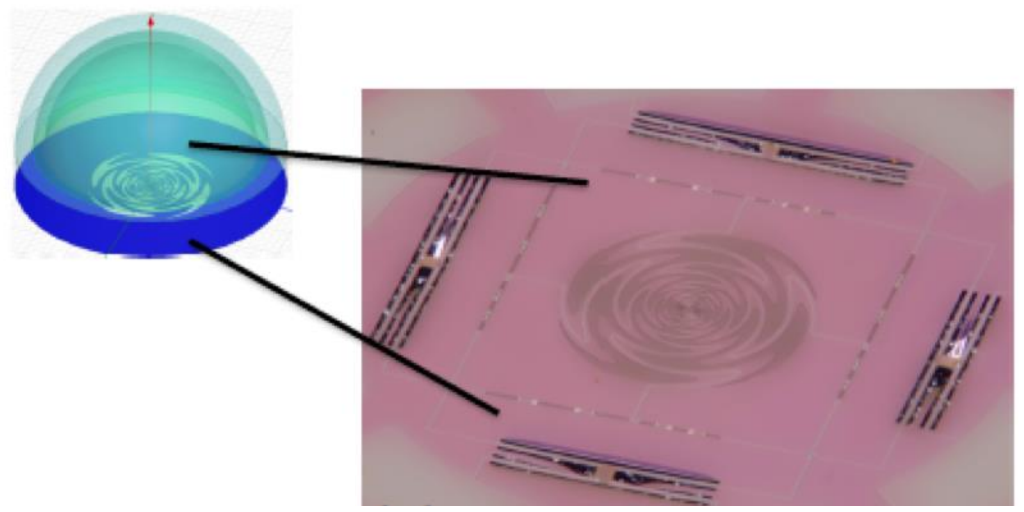

Horn coupled detectors
Platelets

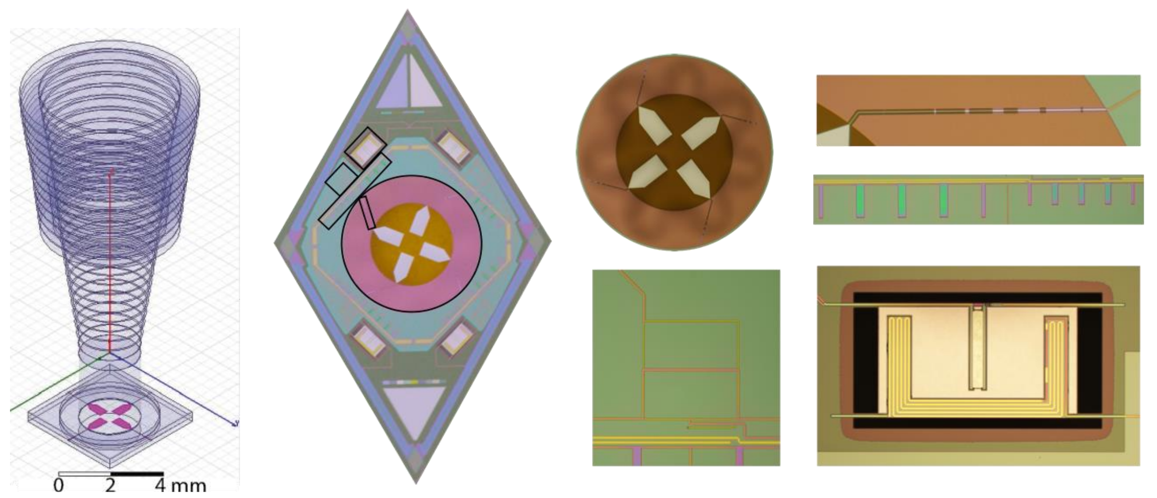

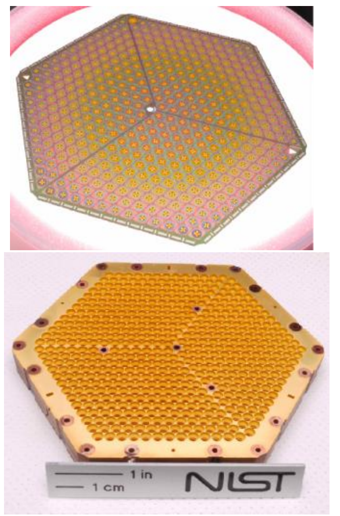

Westbrook+ SPIE 2020

MFT (2.5:1)
89GHz — 225 GHz
2075 detectors
366 Trichroic TES
588 Dichroic TES
Bands: 100, 119, 140, 166, 195

LFT (5.7:1)
34GHz — 161 GHz
Bands: 40, 50, 60, 68, 78, 89, 100, 119, 140
68, 78, 89
1258 detectors
2 x (65 + 155) Trichroic TES

HFT (2.7:1)
166 GHz — 448 GHz
Bands: 195, 235, 280, 337, 402
1355 detectors
2 x 255 Dichroic TES
338 Monochromatic TES

LiteBIRD cryogenic system

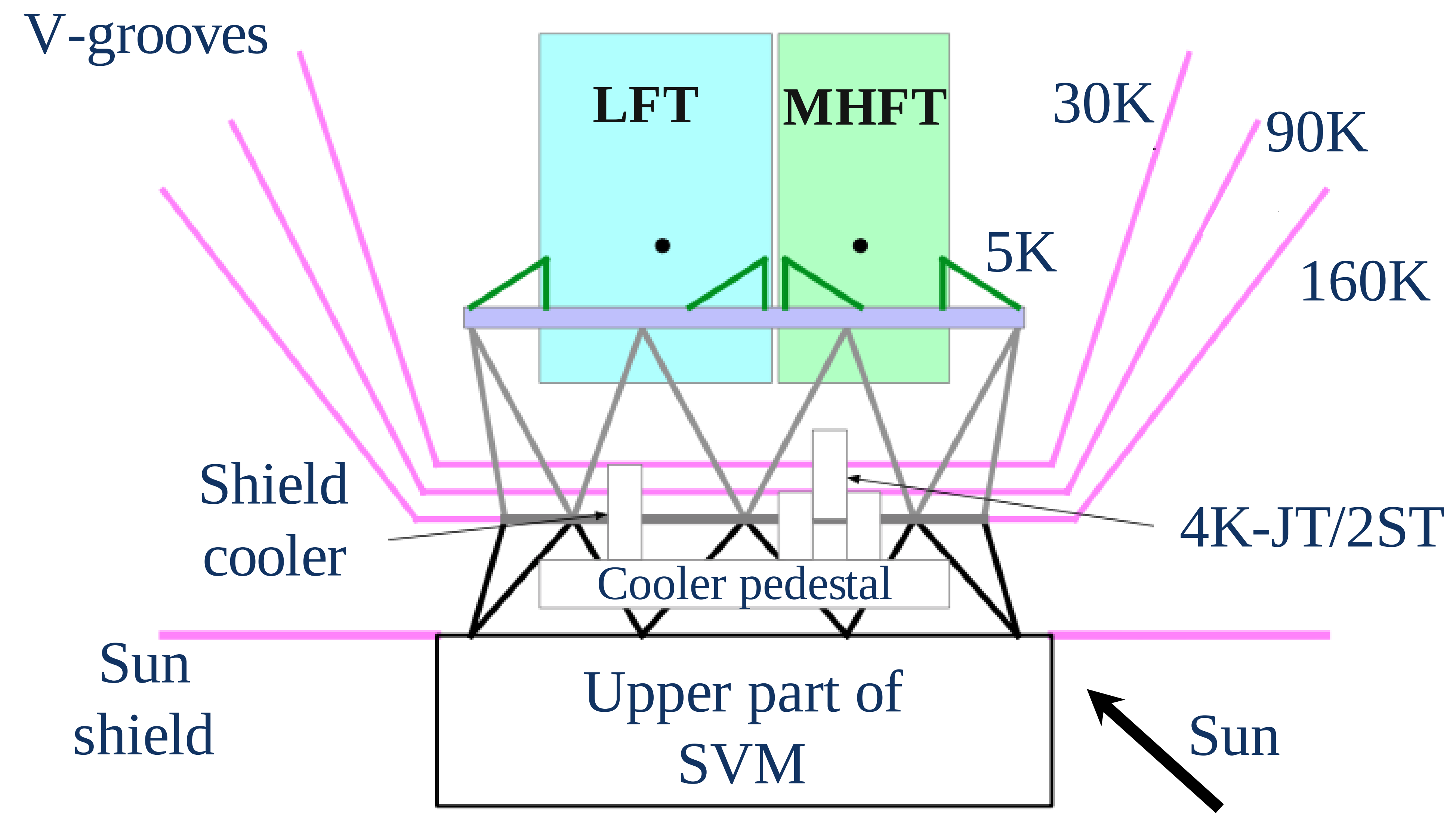

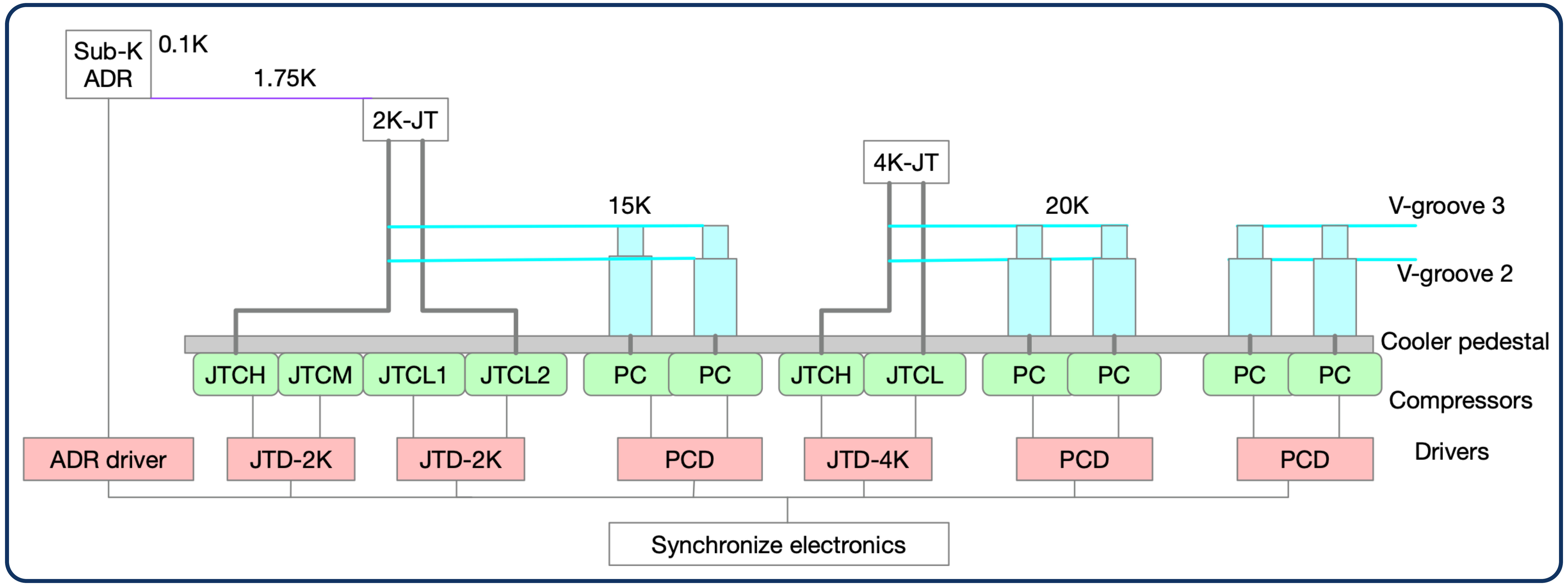

- Continuous cooling at 100 mK
- High stability on telescopes at all stages

LiteBIRD readout system

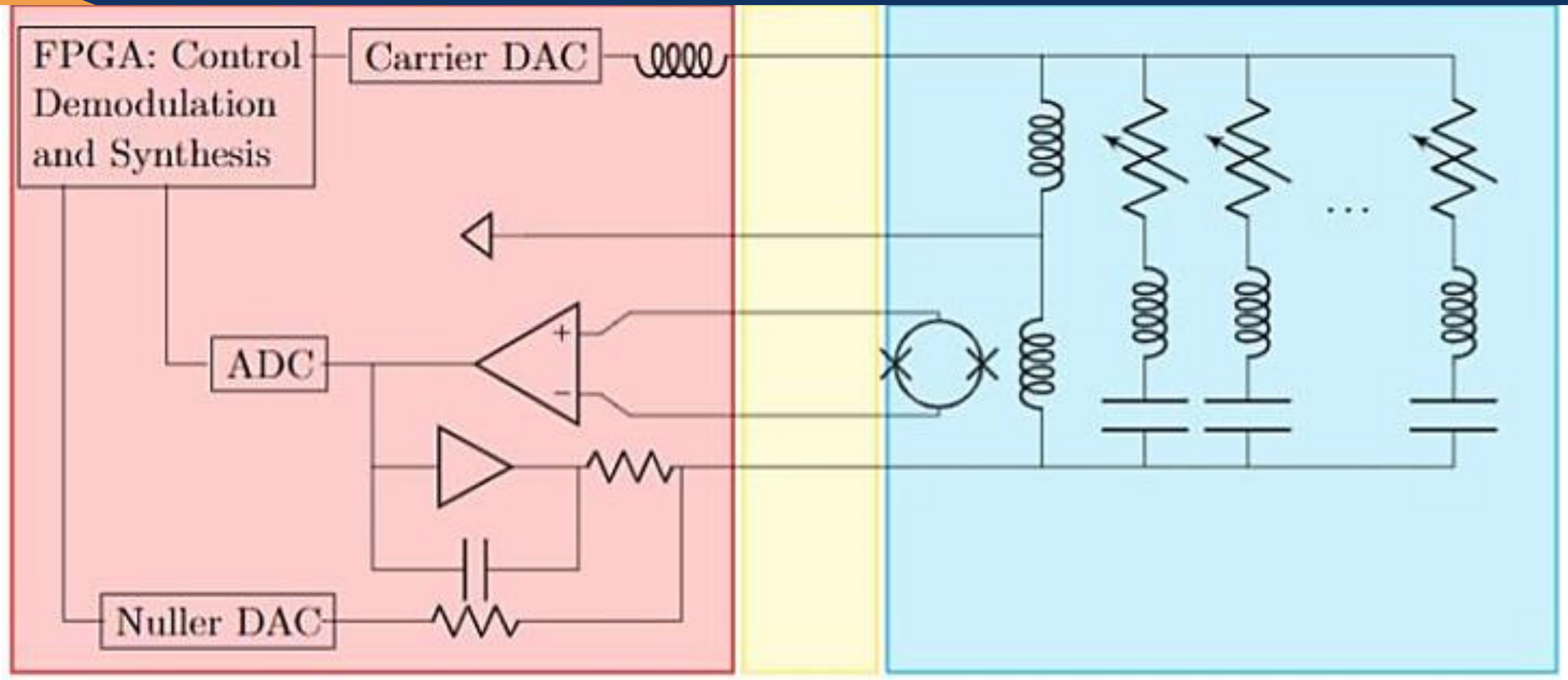

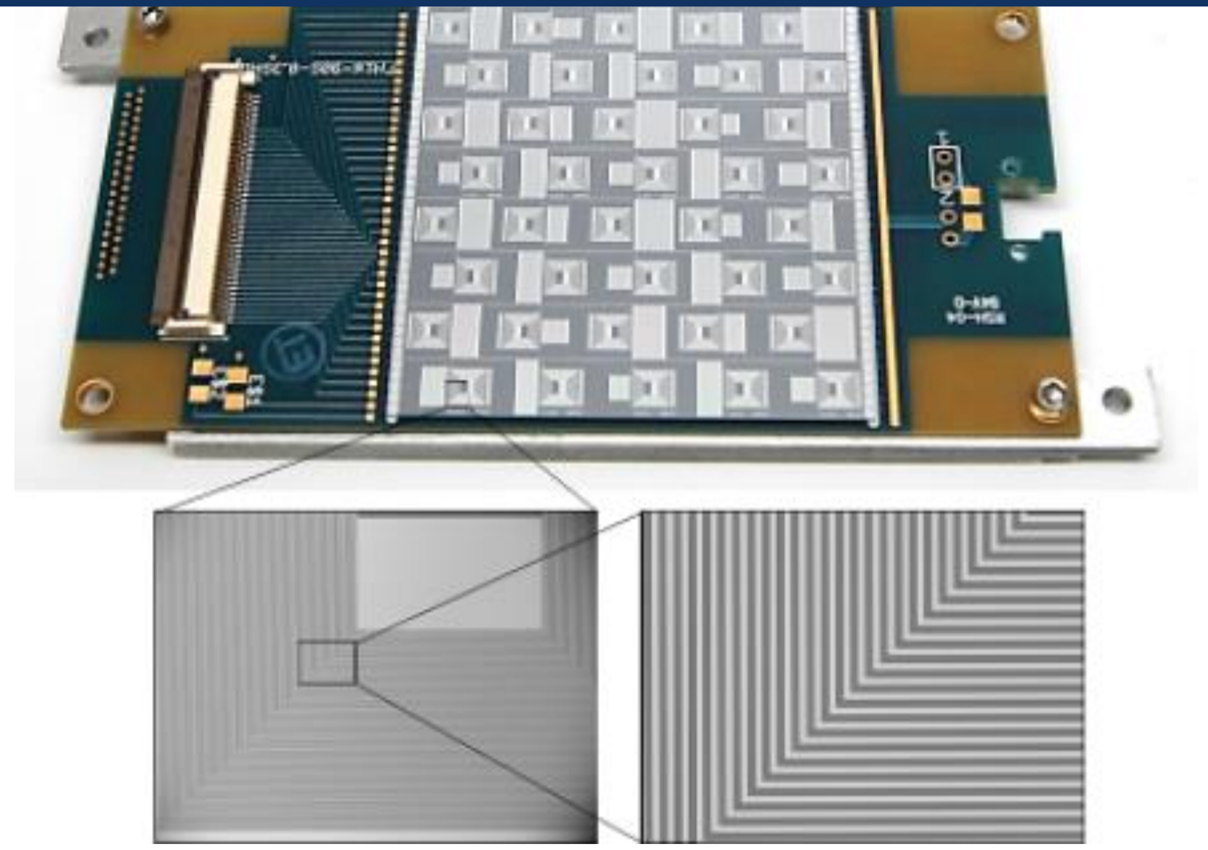

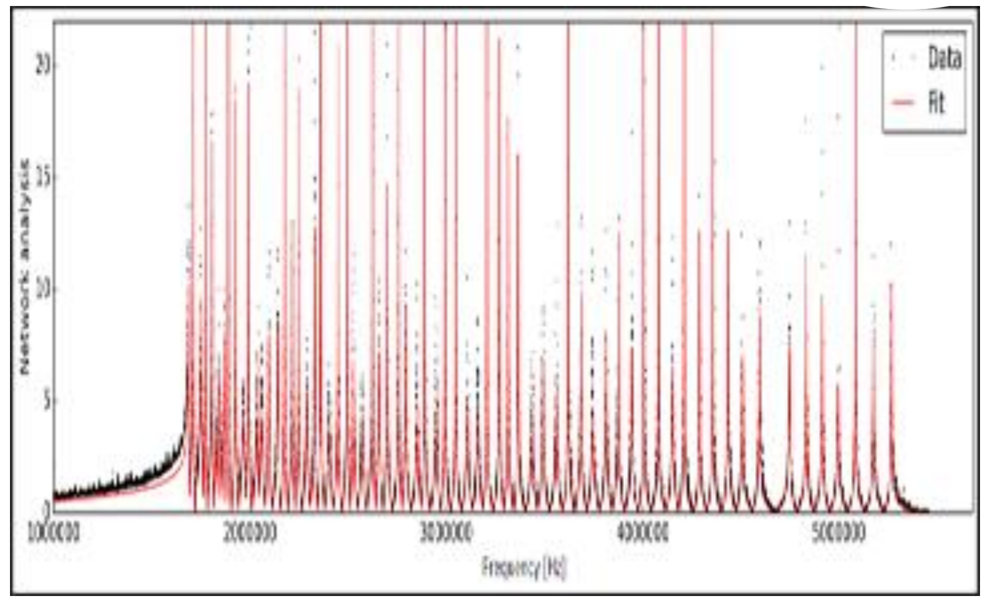

Cold Readout LC filters for MUX

- Digital frequency multiplexing (DfMux) readout technology enables the readout of many Transition Edge Sensors (TES) with fewer components and a low wire count.
- Superconducting resonators are used to assign unique frequency channels to the TES sensors.
- The signal is read out using a low-noise SQUID amplifier and an FPGA controller.
- This approach saves on mass, volume, power consumption, and cost.
- The technique draws its heritage from ground-based CMB experiments.

SQUID controller board

SQUID controller assembly

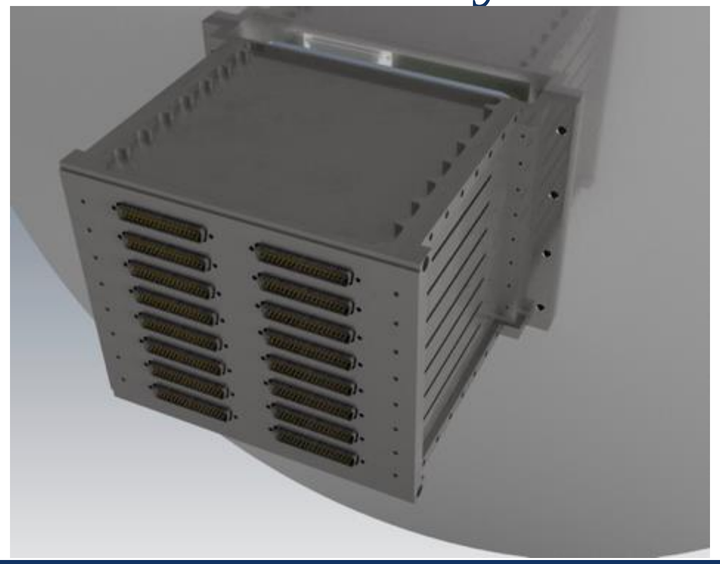

Digitizer assembly

Signal Processing Unit

Digitizer assembly

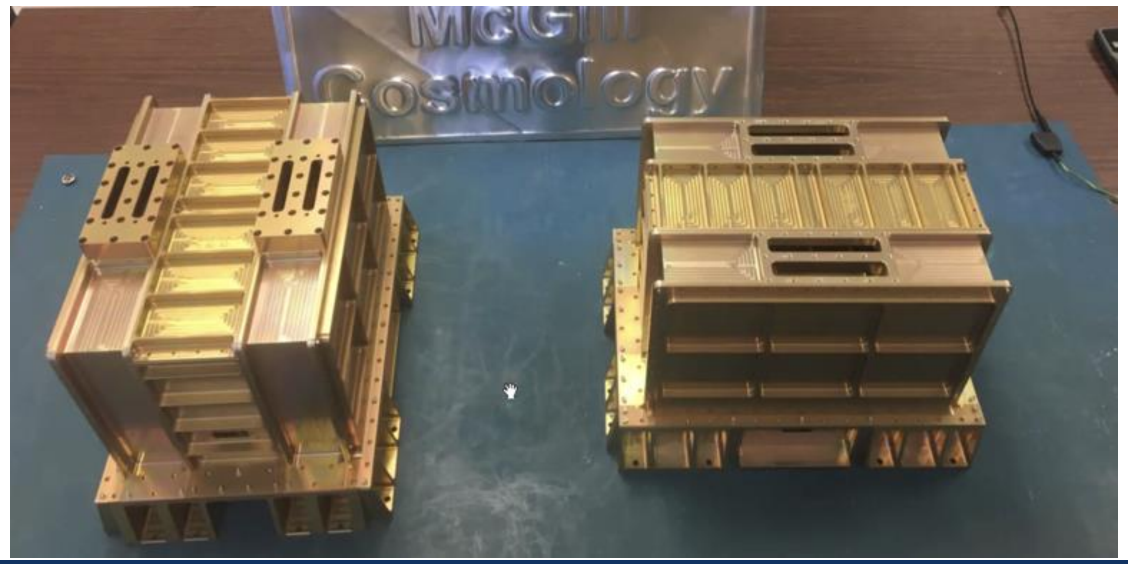

Polarization Modulation Unit (PMU)

- Rotating a birefringent plate to modulate polarization
- The first sky-side optical element

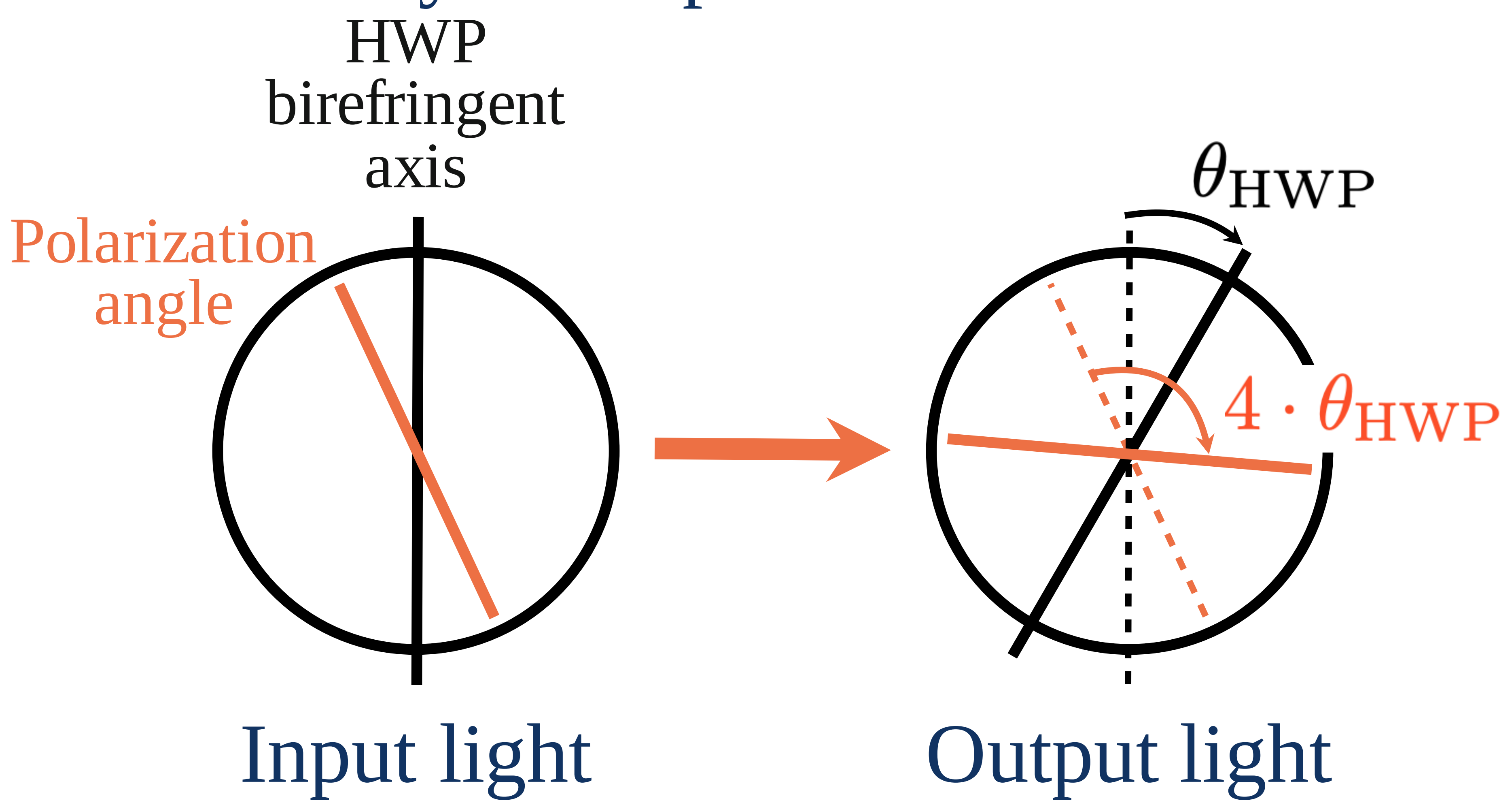

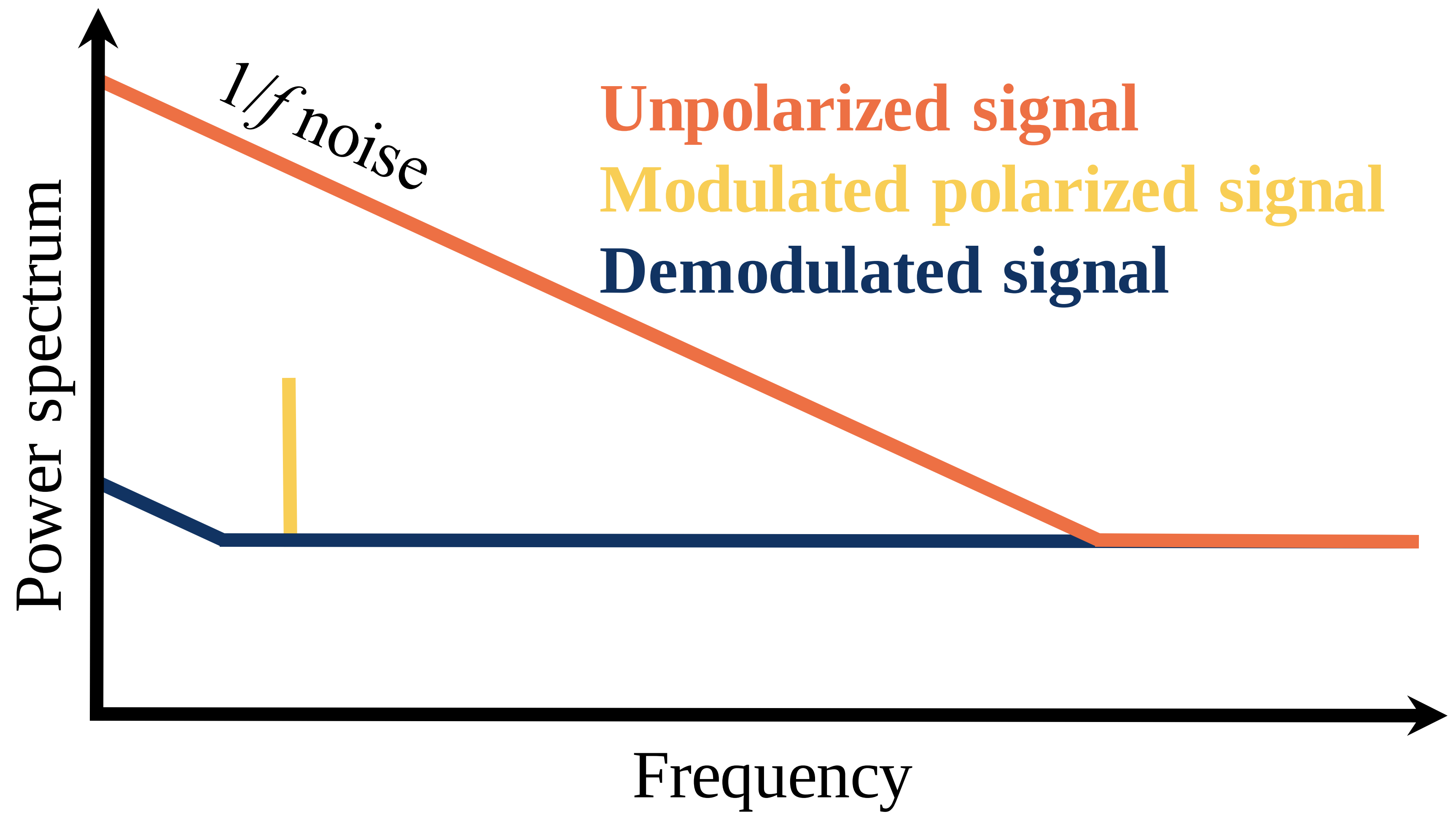

Sakurai+2020 Komatsu+2020
Toda+2020 Columbro+2020 Sugiyama+2020

- LFT PMU BBM at Kavli IPMU:

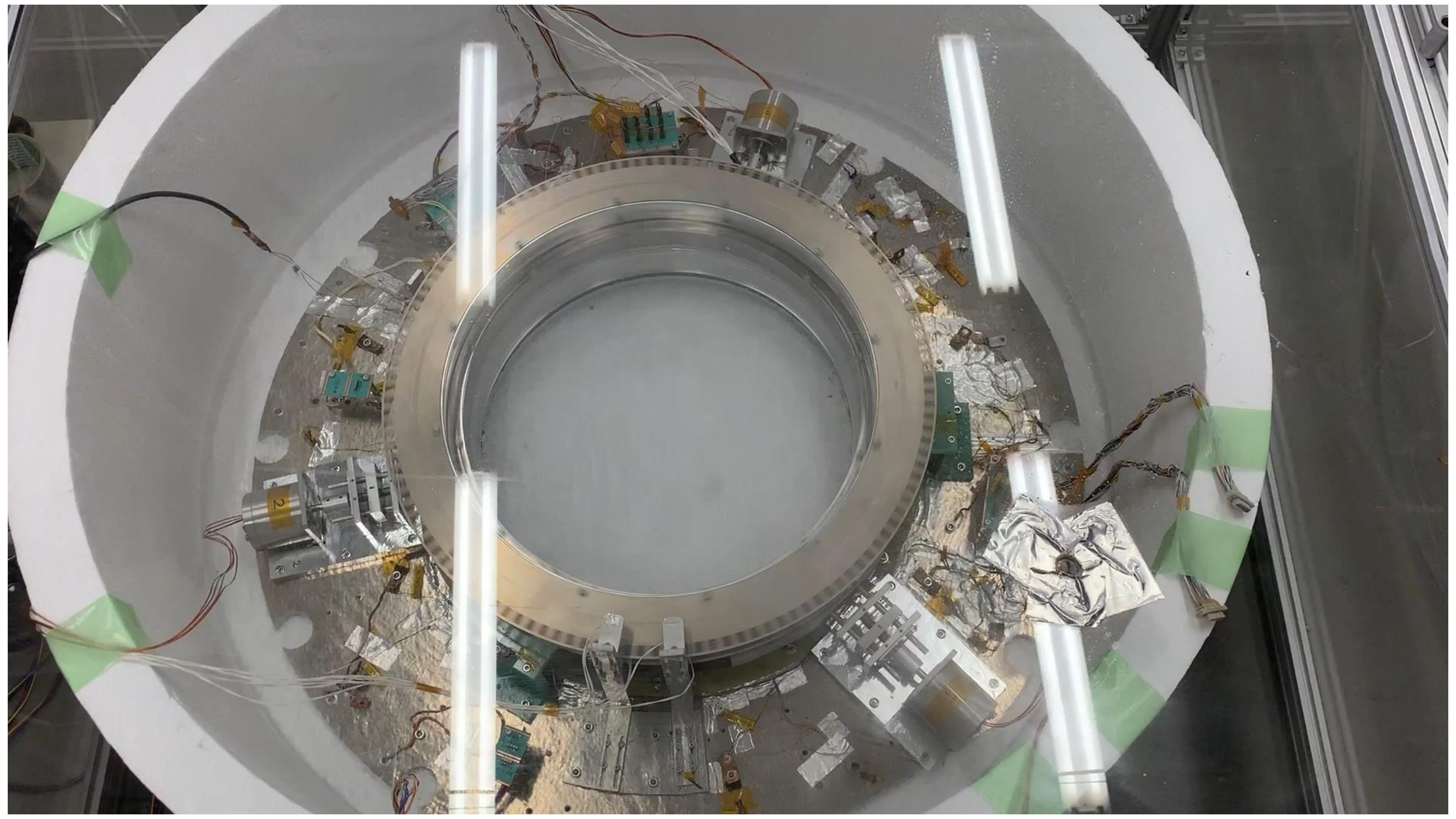

- Rotation test of superconducting magnetic bearing system in the 4K cryostat
- Stable rotation at cryogenic temperature (< 10 K)

Foreground cleaning

Foreground modeling

- **Synchrotron**: curved spectrum (AME is absorbed in the curvature)

$$[Q_s, U_s](\hat{n}, \nu) = [Q_s, U_s](\hat{n}, \nu_\star) \cdot \left(\frac{\nu}{\nu_\star}\right)^{\beta_s(\hat{n}) + C_s(\hat{n}) \ln(\nu/\nu^c)}$$

- **Dust**: modified blackbody

$$[Q_d, U_d](\hat{n}, \nu) = [Q_d, U_d](\hat{n}, \nu_\star) \cdot \left(\frac{\nu}{\nu_\star}\right)^{\beta_d(\hat{n}) - 2} \frac{B_\nu(T_d(\hat{n}))}{B_{\nu_\star}(T_d(\hat{n}))}$$

↓

8 parameters in each sky patch

- "**Multipatch** technique" (extension of xForecast), to account for spatial variability. $12 \times (N_{side})^2$ patches ⇒ 6144 parameters with $N_{side} = 8$

Impact of foregrounds residual

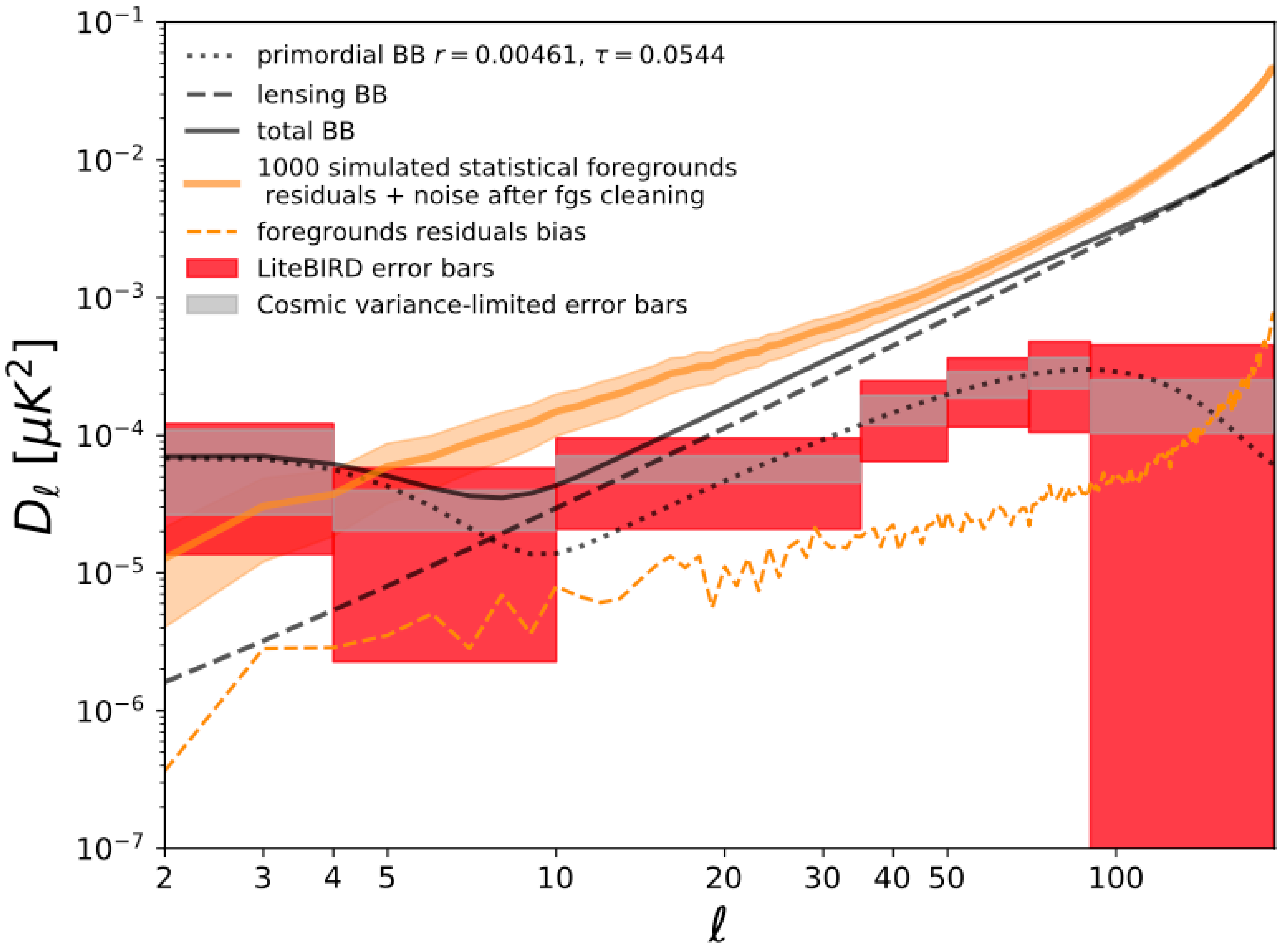

Foreground cleaning

- "Multipatch technique" (extension of xForecast)
- Distribution of the recovered *r* in 1000 simulations with input *r* = 0, with and without foreground residuals
- Bias from foreground (PySM `d1s1`) residuals is found to be small
- Final value: ***r* = (3.3 ± 6.2)×10^{-4}**